Selectivity of major isoquinoline alkaloids from *Chelidomium majus* towards telomeric G-quadruplex: A study using a modified transition-FRET (t-FRET) assay.

Sakineh Kazemi Noureini[a,*], Hosein Esmaeili[a], Farzane Abachi[a], Soraia Khiali[f], Barira Islam[b], Martyna Kuta[d], Ali A. Saboury[e], Marcin Hoffmann[d], Jiri Sponer[b,c], Gary Parkinson[f], Shozeb Haider[f,*]

[a] Deptartment of Biology, Faculty of Basic Sciences, Hakim Sabzevari University, P.O.Box: 397, Sabzevar, Iran
[b] Institute of Biophysics, Academy of Sciences of the Czech Republic, Královopolská 135, 612 65 Brno, Czech Republic
[c] Central European Institute of Technology (CEITEC), Masaryk University, Campus Bohunice, Brno, Czech Republic
[d] Adam Mickiewicz University, Poznan, Poland
[e] Institute of Biochemistry and Biophysics, University of Tehran, Tehran, Iran
[f] UCL School of Pharmacy, Brunswick Square, London, UK

*** Corresponding Authors:**
Sakineh Kazemi Noureini
Deptartment of Biology, Faculty of Basic Sciences, Hakim Sabzevari University,
P.O.Box: 397, Sabzevar, Iran
Email: kazemibio@gmail.com
Tel.: +98-5144013012
Fax: +98-5144013365.

And

Shozeb Haider
UCL School of Pharmacy
29-39 Brunswick Square
London WC1N 1AX
UK
Email: Shozeb.haider@ucl.ac.uk
Tel.: +44-2077535883

Structured Abstract

Background

Natural bioproducts are invaluable resources in drug discovery. Isoquinoline alkaloids of *Chelidonium majus* constitute a structurally diverse family of natural products that are of great interest, one of them being their selectivity for human telomeric G-quadruplex structure and telomerase inhibition.

Methods

The study focuses on the mechanism of telomerase inhibition by stabilization of telomeric G-quadruplex structures by berberine, chelerythrine, chelidonine, sanguinarine and papaverine. Telomerase activity and mRNA levels of hTERT were estimated using quantitative telomere repeat amplification protocol and qPCR, in MCF-7 cells treated with different groups of alkaloids. The selectivity of the main isoquinoline alkaloids of *Chelidonium majus* towards telomeric G-quadruplex forming sequences were explored using a sensitive modified thermal FRET-melting measurement in the presence of the complementary oligonucleotide CT22. We assessed and monitored G-quadruplex topologies using circular dichroism (CD) methods, and compared spectra to previously well-characterized motifs, either alone or in the presence of the alkaloids, Molecular modeling was performed to rationalize ligand binding to the G-quadruplex structure.

Results

The results highlight strong inhibitory effects of chelerythrine, sanguinarine and berberine on telomerase activity, most likely through substrate sequestration. These isoquinoline alkaloids interacted strongly with telomeric sequence G-quadruplex. In comparison, chelidonine and papaverine had no significant interaction with the telomeric quadruplex, while they strongly inhibited telomerase at transcription level of hTERT. Altogether, all of the studied alkaloids showed various levels and mechanisms of telomerase inhibition.

Conclusions

We report on a comparative study of anti-telomerase activity of the isoquinoline alkaloids of *Chelidonium majus*. Chelerythrine was most effective in inhibiting telomerase activity by substrate sequesteration through G-quadruplex stabilization.

General Significance

Understanding structural and molecular mechanisms of anti-cancer agents can help in developing new and more potent drugs with fewer side effects. Isoquinolines are the most biologically active agents from *Chelidonium majus*, which have shown to be telomeric G-quadruplex stabilizers and potent telomerase inhibitors.

Keywords: chelerythrine, sanguinarine, berberine, chelidonine, papaverine telomerase, t-FRET, transition, G-quadruplex

Highlights:

- Isoquinoline alkaloids from *Chelidonium majus* bind selectively to telomeric G-quadruplex and inhibit telomerase activity via substrate sequestration
- Selectivity to G-quadruplex studied using a novel, sensitive modified transition-FRET (tFRET) assay in the presence of complimentary oligonucleotide
- The ligands bind to the terminal quartet and maximize π-π stacking interactions in the 3+1 hybrid topology quadruplex

1. Introduction

Bioactive natural compounds have been explored as new agents to combat malignancies, overcome drug-resistance and prevent carcinogenesis [1]. Telomerase is a key target for therapeutic intervention in cancer cells. It has been shown to be selectively inhibited by natural products including berberine, sanguinarine and their derivatives via G-quadruplex (G4) stabilization [2,3]. The extract and derivatives from *Chelidonium majus* have been used in treatment of several malignancies including gastric and breast cancer since 1896 [4-7]. The extract includes several chemically and pharmacologically interesting alkaloids [8], in which the most biologically active components are isoquinolines and their derivatives (Figure 1) [9]. Isoquinolines have shown different cytotoxic mechanisms in several transformed and malignant cell types [9-14]. For example, chelidonine and sanguinarine have shown varying apoptogenic strength without DNA damage [15], while some others have shown radio-protective effects on normal but not cancer cells [16]. Ukarin, a synthetic derivative related to these compounds, has shown selective inhibition of cancer cells, with no significant toxicity in normal cells even at much higher concentrations [17]. Of the several mechanisms, inhibition of telomerase via G4 stabilization remains an attractive proposition.

The enzyme telomerase is over-expressed, by up to a hundred-fold, in more than 85% of cancer cells [18]. It rescues cancer cells from end-replication problem by maintaining telomere length using its intrinsic RNA as the template [19], thus conferring a strong selective advantage for continued growth of malignant cells [20-22]. The guanine-rich, single strand terminal ends of telomeres may fold into a strong and stable intramolecular G4 structures, which prevents accessibility to telomerase [23]. Various strategies have targeted this structure to suppress telomerase activity in rapidly dividing cancer cells [24-26].

One approach put forward by the Neidle group is to stabilize G4 structures using small molecules; thereby preventing access to single stranded telomeric DNA for telomere elongation by telomerase [27]. Our previous screening studies on G4 stabilizing natural agents showed that isoquinoline alkaloids of *Chelidonium majus* could suppress proliferation and active telomerase content of cancer cells [13, 14, 28]. Various sets of isoquinolines like berberine have been studied for their mode of interactions with telomeric G4 DNA including their stoichiometry [29] and energetics of binding [30]. Molecular modeling and NMR spectroscopic data are available on berberine and

sanguinarine, highlighting their selectivity for G4 DNA and the dominant role aromatic moieties play in G4 binding [2,31].

In this study, we focused our investigation on the mechanisms of telomerase inhibition by stabilizing G4 DNA via berberine, chelerythrine, chelidonine, sanguinarine and papaverine. We explored hTERT expression level in parallel with telomerase activity in treated cells. The probable direct interaction of the compounds with telomerase ribonucleoprotein were studied using ligand-TRAP experiments and the selectivity of ligand binding to telomeric G4 DNA versus ds-DNA was explained by classical and a novel modified thermal FRET-melting assays. Sequence dependence G4 topology, associated ligand preference and thermal stability to various alkaloids was also monitored using CD methods.

2. Material and methods

2.1. Cell culture and cytotoxicity

Human breast adenocarcinoma cell line MCF7 (ACC115 from DSMZ) were maintained in 75 cm^2 culture flasks in DMEM, supplemented with 10% heat-inactivated fetal bovine serum, 100 U/ml penicillin, and 100 µg/ml streptomycin (all the materials from PAA, Austria). Cells were grown in 5% CO_2 and 90% humidity at 37°C. Cell viability was evaluated routinely by trypan blue exclusion method using a hemocytometer.

Among the commercially available different classes of isoquinoline alkaloids, 12 pure compounds were purchased from Sigma-Aldrich. Cytotoxicity of the compounds was estimated using MTT method [32]. Briefly, cells in the exponential phase (24 hours after seeding in 96 well plates 10000 cells per well) were incubated with various concentrations of the desired compound freshly prepared from the stock solutions (10 or 50 mM in absolute ethanol). The final concentration of ethanol was always less than 0.1%. After incubation for 48 hours, MTT 3-(4,5-dimethylthiazol-2-yl)-2,5-diphenyl-tetrazolium bromide (Sigma-Aldrich) was added to a final concentration of 0.5 mg/ml to each well. The plate was further incubated for four hours for MTT reduction to formazan purple product through mitochondrial dehydrogenases of viable cells. The absorbance was read at 570 nm using a plate reader (BioTek, USA) after dissolving the formazan product in dimethylsulfoxide containing 10% SDS and 1% acetic acid. The tests were repeated at least 3 times each in triplicates and the LD_{50} values were calculated from dose-response curves using Gen5 version1.06 software.

2.2. Circular dichroism

The oligonucleotide telo-G21 (5'-$GGG(TTAGGG)_3$-3') was purchased from Eurofins Genomics. The sample was first dissolved in water, then diluted to a final concentration of 0.01 mM in buffer consisting of KCl (100 mM) and sodium Cacodylate (10 mM, pH 7.2). The sample was heated at 95°C in the heating block for two minutes and then left cooling overnight at room temperature and then stored at 4°C. The ligands, chelerythrine, papaverine, berberine and chelidonine, were purchased from Sigma-Aldrich, the sanguinarine was purchased from Cambridge bioscience. They were all dissolved in di-methyl sulfoxide (DMSO) at the final concentration of 33 mM and then

stock solutions of ligands at the concentrations of 0.01 mM, 0.1 mM and 1 mM were prepared doing several dilutions with water.

Twenty solutions (final volume 0.2 ml) of complexes DNA-ligands were prepared adding DNA solution (final concentration 0.001 mM), in sodium Cacodylate buffer (final concentration 10 mM, pH 7.2 and KCl 100 mM), water to take to volume and the right amount of ligand solution to obtain the final concentrations of 1 mM, 0.1 mM, 0.01 mM and 0.001 mM for each ligand, and two more solutions of complex DNA-chelerythine were prepared at these ratios: 1:4 and 1:2. The solutions were incubated at 37°C for two hours, then circular dichiroism experiments were carried out on Chirascan Plus using quartz cells of 0.1 cm path length (scan rate 4 s/nm) at 25°C.

2.3. Quantitative Telomere Repeat Amplification Protocol (q-TRAP)

Sub-confluent MCF-7 cells were seeded in 6 well plates and incubated for 48 hours with various concentrations of the test compound. Cells were washed with PBS, lysed according to Kim *et al*. [33] and incubated for 30 min at 4°C. The lysates were centrifuged at 16,000×g for 30 min at 4°C. Protein concentration of supernatant was measured by Bradford method [34]. Q-TRAP assay was performed by real-time SYBR-Green method [35] with small modifications as previously reported [36]. The reaction mixtures including 1X SYBR Green master mix (GenetBio, South Korea), 1 µg protein of cell extract, 10 pmol TS (5'-AATCCGTCGAGCAGATT-3') and 5 pmol ACX (5'-GCGCGGCTTACCCTTACCCTTACCCTAACC-3') primers were incubated for 30 min at 25°C. DNA products from telomerase activity were amplified using the following conditions: The hot-start taq polymerase was activated by heating at 94°C for 10 min followed by 40 cycles of 30 sec at 94°C, 30 sec at 50°C and 45 sec at 72°C with signal acquisition on a real-time thermal cycler Rotor Gene 3000 (Corbett Research). The threshold cycle values (Ct) determined by Rotor Gene 6.01 software were compared with the standard curve generated from serially diluted cell lysate of untreated MCF-7 control. Each experiment included a negative control, which was a reaction mix without cell extract or a heat / RNase-treated sample to inactivate telomerase. This experiment was performed for every test compound in at least three logically independent repeats with three or more samples per point.

For ligand-TRAP tests, the reactions were incubated with the desired concentrations of alkaloid before or after telomerase activity as explained above [37] with small modifications. Briefly, a master mix of q-TRAP reaction including MCF-7 cell lysate was prepared and aliquoted to two sets on ice (A and B). Various concentrations of the desired alkaloid were added to samples of set A and incubated for 30 minutes on ice. Then all samples of both sets were incubated for 20 min at 24°C for extending TS primer by telomerase. All the samples were put back on ice and the same concentrations of alkaloid as set A was added to the samples of set B. Only Taq polymerase will be exposed to the alkaloids in this set. The amplification and quantification were done as described in the previous section. This experiment has been repeated at least three times, and each repeat included triplicate samples for each concentration of the alkaloid. Traces of RNase contamination that potentially can give rise to false positive results was checked by incubating total RNA with aliquots of the alkaloids for 0 or 30 min at room temperature followed by electrophoresis in agarose gel.

2.4. Total RNA isolation, cDNA synthesis and Real-time PCR

Total RNA was isolated from the control and treated MCF-7 cells using RNX-Plus solution (SinaClone BioScience, Iran) according to the manufacturer's instructions. cDNA synthesis was performed on 2 μg of each sample using MMULV reverse transcriptase (Vivantis, Korea). Expression levels of the hTERT and β2 microglubolin genes were detected by quantitative reverse transcription polymerase chain reaction (qRT-PCR) that used specific intron-spanning primers as explained above [36]. Briefly, 1 μl of each cDNA sample was subjected to PCR-amplification reaction including SYBR Green PCR Master Mix (GenetBio, Korea) and 5 pmol of each primer. Relative mRNA copy number of hTERT gene to that of the housekeeping gene, β2 microglubolin, was compared among the control and treated samples using the related standard curves calculated by Rotor-Gene 6.01 software.

2.5. Thermal FRET and CD analysis

The probable interaction of the alkaloids with telomerase substrate and interference with the enzyme activity was estimated through a simple thermal melting experiment based on Guedin *et al*., 2010 [38] with small modifications. By using these methods we can demonstrate the structural stabilization effect of the alkaloids on a dual-labeled fluorescence synthetic oligonucleotide of

human telomere sequence rich in guanine, F21T (FAM 5'-GGG(TTAGGG)$_3$-3' TAMRA) and native telo-21G (5'-GGG(TTAGGG)3-3'), which inherently fold to an intramolecular G4 DNA. Fluorescence intensity of F21T was measured while heating gradually from 30 to 98°C at the rate of 1°C/min while for CD from 37 to 98°C at the rate of 1min/°C. G4 DNA structures unfold at high temperatures. The temperature at which the transition from folded to unfold structure occurs, correlates to the melting temperature (T_m). The ligands that preferentially bind to and stabilize the folded state of F21T and unlabeled telo-21G increase its T_m.

FRET fluorescence intensity increased in an almost two state denaturation pattern. Briefly, F21T at final concentration of 0.25 μM was heated at 95°C for 10 min, immediately chilled on ice and incubated at 37°C for 2 h in presence of sodium cacodylate (10mM) and KCl (100 mM); and equimolar concentration of the desired alkaloid. Fluorescence intensity of F21T was detected using Rotor Gene 3000 real-time thermal cycler (Corbett Research) as the temperature was increased at the rate of 1°C/min. The correlated melting temperatures were calculated by using differential fluorescence intensity of F21T as a function of temperature with Rotor Gene software version 1.06 and compared with that of the oligonucleotide alone. The denaturation pattern monitored by CD shows a single state melt unmodified by the presence of ligands (Figure 5B). For CD thermal experiments the materials were prepared as previously described, where the signals were collected after each step of increasing temperature by the rate of 1°C/min from 37 to 90°C from 220 nm to 320 nm (scan rate 0.5 s/nm).

Another set of FRET experiments, called transition FRET (t-FRET), were conducted with a similar protocol except that the reactions contained equimolar concentrations of the complementary oligonucleotide CT22 (CCCTAA)$_3$CCCT and F21T. After initial heating to unfold the oligonucleotides and immediately chilling on ice, folding to duplex or quadruplex can occur competitively by incubating at 37°C. The duplexes will cause strong fluorescence intensity of F21T due to the greater distance between the dyes in duplex structure relative to quadruplex structure. This set of experiments may evaluate the binding specificity of the compounds to quadruplex structure of F21T with low fluorescence. The higher fluorescence intensity at the start point of FRET measurement demonstrates priority of unfolded state of F21T, which participates in duplex DNA with the CT22 oligonucleotide. However, in presence of ligands, lower fluorescence

intensity at the beginning of the FRET measurement can be explained with folded state of F21T into quadruplex that is stabilized with high affinity of the ligand to this structure. In such cases, the melting temperature is expected to be higher than control samples.

2.6. Molecular Dynamics (MD) simulations

The hybrid 3+1 topology of intramolecular telomeric quadruplex (PDB id 2MB3) was used as the starting point to study G4-ligand interactions [64]. The docking and molecular dynamics protocol was adapted from Ohnmacht et al. [39].

The chemical structures of the ligands were sketched, built and docked using ICM-Pro software [40]. The charges were assigned using the ICFF force field. Grid maps were made that encompassed the terminal quartet. Docking was done using the automated docking module in ICM-Pro software, employing the default parameters. The final docked conformation was chosen based on the strongest binding energy between the docked ligand and the quadruplex. The docked complex for each ligand was chosen as the starting structure for MD simulations.

The stability of ligand-G4 complexes were assessed by MD simulations. The complexes were set up using the xleap module in the AMBER14 molecular dynamics package [41]. The simulations were carried out in parmbsc1 version of Cornell et al. force field with X_{OL4} modifications [42-44]. The system was solvated in a periodic box whose boundaries extended at least 10 Å from any solute atom. The complexes were neutralized by adding K^+ ions and Amber-adapted Joung and Cheatham parameters specific for TIP3P waters were used [45].

The complexes were first minimised using 1000 steps of steepest descent, followed by 1000 steps of conjugate gradient minimisation. A 300 ps of MD equilibration was run in which the G4 was restrained while the ions and water were allowed to equilibrate. The systems were gently heated from 0 K to 300 K with a time step of 0.5 ps followed by another round at constant pressure at 300 K for 1 ns. The constraints were gradually relaxed until no constraints were applied on the systems. The final production MD run was carried out for 250 ns using ACEMD [46]. The default parameters were used and included 10Å non-bonded cut-off,

0.0001Å tolerance was allowed for the SHAKE algorithm, an integration step of 2 fs, constant pressure of 1 ATM at 300 K temperature. The frames were collected every 20 ps and the analysis of the trajectory was performed using the CPPTRAJ module of AMBER. VMD was used to visualise the trajectories [47] and the figures were made in the ICM-Pro software.

2.7. Statistical analysis

Statistical analysis was performed by using one-way ANOVA test and a $p < 0.05$ was considered as the cut off for significant difference.

3. Results

3.1. The alkaloids showed different level of cytotoxicity in cell culture

MTT experiments in 48 h treated MCF-7 cells with berberine, chelidonine, sanguinarine and chelerythrine (Figure 1) estimated LD_{50} values as 54, 8, 3 and 2.5 μM respectively. The cytotoxic effects of all of the compounds are strongly time- and dose-dependent. The rate of cell death increased sharply even at very low concentrations, while it reached a gradual rate around and beyond the LD_{50} (Figure 2). Papaverine was the least cytotoxic compound amongst these alkaloids. Its 48h LD_{50} has been previously reported to about 120 μM in MCF7 [48] and HepG2 cells [49].

3.2. Isoquinoline alkaloids generally do not change the CD signature of telo-21G in annealed in either sodium or potassium.

A positive peak at 251 nm and two small maxima at 271 and 288 nm were seen in the CD spectrum of the human telomeric sequence telo-21G (Figure 3), similar to when annealed in either potassium or sodium buffers (data not shown). The human telomeric sequence may adopt an anti-parallel, parallel, or 3+1 hybrid G-quadruplex topologies. The observed CD spectrum suggests a mixture of G-quadruplex conformations with different proportions or an interchangeable base stacking within the structures [47,65]. However in presence of the ligands the signature remained unchanged except for a slightly stronger intensity of the maxima at 288 nm and a small decrease in maxima at 271 than the telo-21G alone except for chelerythrine. The strongest changes were observed in presence of chelerythrine followed by modest changes for berberine, chelidonine, sanguinarine, and papaverine. Chelerythrine at the molar ratio of 1:4 ligand:telo-21G made as

large as ~12% stronger maxima at 288 and ~16% decrease in minimum at 238 nm than telo-21G alone (Figure 3). A moderate shift about 3.8 and 5.4°C in $T_{1/2}$ of telo-21G in presence of chelerythrine at molar ratio of 1:4 and 1:2 ligand: telo-21G was detected in thermal CD experiment.

3.3. Telomerase activity was suppressed by alkaloids to various extents

Quantitative telomere-repeat amplification protocol (qTRAP) measurements assessed IC_{50} levels of each compound in samples containing equal amounts of total protein (Figure 4). A dose-dependent inhibitory effect was seen in MCF-7 cells treated with the alkaloids. The concentration of the alkaloid that leads to 50% telomerase inhibition in MCF-7 cells after 48 hours incubation, its $IC_{50,}$ was estimated as 27, 1.25, 1, 1.25 and 60 μM for berberine, chelerythrine, chelidonine, sanguinarine and papaverine respectively. In the treated cells berberine at LD_{50} concentration (estimated using MTT assay) suppressed telomerase activity down to 10% of untreated cells. The LD_{50} concentration of chelerythrine showed 60% inhibition of telomerase in the qTRAP assay, although it was able to inhibit telomerase even at a very low concentration in a dose-dependent manner. Telomerase activity was strongly inhibited at very low concentrations of chelidonine or sanguinarine and progressed to almost complete inhibition at their respective LD_{50}.

3.4. Chelidonine decreased hTERT expression significantly

All of the studied alkaloids showed a decreasing effect on the relative hTERT mRNA levels in treated MCF-7 cells (Figure 4, black lines). Berberine, inhibited hTERT transcription down to about 18 ± 5.2% of untreated control cells at 3 μM and with no further decrease up to its LD_{50} value of 54 μM. However, chelidonine showed a significant suppression of hTERT transcription. The quantitative real-time RT-PCR technique estimated the strongest decrease in mRNA level of hTERT in MCF-7 cells 48 h treated with 8 μM chelidonine to 3.5 ± 1.5 % of untreated controls. A reduction of hTERT mRNA level to ~60% and less than 40% of untreated cells was observed when the cells were treated with 0.1 and 1 μM of chelidonine, respectively (Figure 4). Chelerythrine and sanguinarine reduced hTERT transcription to 35 ± 3.2% and 32 ± 3.3% of untreated controls at their respective IC_{50} values.

3.5. Chelerythrine showed the strongest interaction with G4 structure

Thermal FRET analysis of the double-labeled oligonucleotide F21T showed different T_m for G4-alkaloid complexes, indicating that the complexes tested here had different stabilities (Figures 5 and 6B). The T_m values of F21T in 100 mM sodium cacodylate buffer containing 100 mM KCl were calculated at 73°C using dF/dT curves by Rotor-Gene 6.01 software.

The significant high Tm measured for F21T in presence of Chelerythrine and Sanguinarine indicated a strong binding with telomeric G4 structures. Chelerythrine showed the strongest interaction with F21T; as it increased the melting temperature by ~6 °C at equal concentration of F21T and chelerythrine (Figures 5A and 6B green line). Sanguinarine also showed strong binding to F21T, although it was weaker than chelerythrine (Figure 5A and 6B orange line). The ΔT_m caused by sanguinarine on F21T was about 3°C at equimolar concentration. However, berberine, cheldionine and papaverine did not increase the melting temperature of F21T at 1:1 concentration ratio (Figures 5A and 6B; the dark blue, red and blue curves respectively). This suggests a very weak interaction between these alkaloids and F21T. The interaction of the ligands with the unlabeled telo-21G and its stabilization as monitored by $CD_{290\ nm}$ melting shows a similar overall pattern from strong binding to weaker interactions (Figure 6A; the same colors as 5A and 6B). Again chelerythrine shows the strongest interaction, inducing a ΔT_m of 18°C at 100/1 with berberine second at 12°C, both cheldionine and papaverine were the weakest.

3.5.1. G4-duplex transition in the presence of ligands

The specificity of interactions of alkaloids with G-rich F21T oligonucleotide was verified by performing G4-duplex transition experiments in the presence of the complementary oligonucleotide CT22 using a modified thermal FRET method. In these experiments, equimolar solutions of both, F21T and CT22, were first boiled at 95°C for 10 min followed by immediate chilling on ice. Incubating the mixture of oligonucleotides at 37°C allows folding of either duplex or quadruplex structures. A duplex structure will be preferred in the absence of a quadruplex stabilizing ligand. Formation of the folded structure in G-rich strand will be detectable by lower fluorescence intensity than control at the beginning of heating step in FRET measurements. In the absence of any alkaloid, an equimolar mixture of F21T and CT22 showed a sigmoidal curve

starting with high fluorescence intensity at the beginning of FRET measurements (because of flurophore dye separation by duplex formation) followed by a clear transition step, marked as "**a**" (Figure 5A, middle), that correlated with melting temperature of the double helix structure. However, when the strands are separated (at least a fraction of) the G-rich strand F21T oligonucleotide can fold into G4 structure (denoted as "**GQ**" in the curve). By continued heating, a second transition step occurs by denaturing the quadruplexes and if any suitable ligand stabilizes this G4 structure, a ΔT_m will be observed, marked as "**b**" in the curve (Figure 5B, middle).

Folding of F21T in the presence of any ligand will lead to fluorescence quenching. On the other hand, if the ligand strongly interacts with the duplex and stabilizes it, no such quenching will occur and probably a positive ΔT_m is recorded in transition step "a". Meanwhile the ligands that interact with G4 structure may quench fluorescence leading to lower fluorescence intensity, G4 formation in F21T at lower temperature and a negative ΔT_m in transition step "a". This modified FRET-melting method may help to differentiate between quadruplex and duplex specific ligand binding. None of the alkaloids in this study stabilized F21T:CT22 duplex, however chelerythrine and sanguinarine exhibited strong fluorescence quenching at the beginning of the heating and a negative ΔT_m in the transition step "a" (Figure 5A, middle). While other ligands made no changes on both transition steps. Chelerythrine and in a lesser amount sanguinarine increased T_m of F21T as observed in transition step "b". This suggests the stronger effects of these two benzophenanthridine alkaloids on telomeric G4 stabilization.

Chelidonine did not show any considerable changes in melting temperature of F21T, in presence or absence of CT22, although it has previously been shown to inhibit telomerase [12]. Chelerythrine and sanguinarine exhibited a significant stabilization effect on telomeric G4 structure even in the presence of the complementary strand, CT22. In the presence of equimolar concentration of these alkaloids, the fluorescence intensity of F21T largely decreased at the beginning of the heating step of the FRET measurements. The lower fluorescence intensity reasonably correlated with the folded state of F21T quadruplex. Both chelerythrine and sanguinarine strongly favored F21T folding into G4 than hybridizing with CT22 to a duplex DNA. The lowest fluorescence intensity of F21T was detected in the presence of equimolar concentration of chelerythrine and sanguinarine which caused a ~50 and 40% decrease in fluorescence intensity

respectively. Berberine exhibited a weaker quadruplex stabilizing effect than chelerythrine and sanguinarine, while reducing the fluorescence intensity of F21T by about 30%. Papaverine and cheldionine did not show any significant ΔT_m in F21T similar to the classic FRET-melting experiments.

The second transition step "b" was almost the same as observed in classical FRET-melting experiments (without the complementary CT22) and the T_m values are almost the same (it was highlighted with red rectangle for berberine in Figure 5B). In summary these observations support the more selective interaction of chelerythrine than sanguinarine and berberine with telomeric sequences.

3.5.2. Molecular dynamics of telomeric-G4 in complex with isoquinolines

Since no structural data of the studied complexes is available, automated ligand docking and MD simulations were carried out to examine the plausible binding features of the ligands with the G4. The binding energies in kcal/mol, calculated after docking the ligands to the quadruplex were in the following order:

Chelerythrine (-29.5) > Berberine (-25.6) > Sanguinarine (-23.6) > Chelidonine (-19.6) > Papaverine (-16.6)

The final configuration of the systems, after 250 ns MD run revealed that the ligands stacked on the quartet with the chromophore maximizing the π-π stacking interactions. The nitrogen in the ligand molecules exhibited a preference to position on top of central electronegative channel that runs through the G4 (Figure 7). The final results from the MD simulations of the complexes are presented in the Supplementary data section.

3.6. The alkaloids generally inhibited both telomerase and Taq polymerase

Ligand-TRAP assay carried out in the presence of chelerythrine, berberine and sanguinarine showed that the alkaloids inhibited telomerase by varying degrees (Figure 8). The effect was not specific to telomerase as similar effect was observed when the alkaloids were added after telomere elongation, in which only the Taq polymerase was active. Thus both telomerase and Taq

polymerase were inhibited by chelerythrine, sanguinarine and berberine. It suggests that strong interaction of these alkaloids with G-rich telomeric sequences, as seen in thermal FRET experiments, is most likely by interfering with both telomerase and Taq activity. Telomerase inhibition appears after a few rounds of primer extension activity of the enzyme by adding the TTAGGG repeats, which adopts G4 structure. The strong interaction of alkaloids may restrict access to the substrate. However in presence of chelerythrine, telomerase was more inhibited than taq polymerase, as incubation with chelerythrine before substrate extension by telomerase showed less TRAP products than incubation after that (Figure 8). No significant reduction in activity of telomerase and/or Taq polymerase was observed in our ligand-TRAP experiments when incubated with chelidonine (data not shown).

4. Discussion

Discovery of new drugs that are selectively cytotoxic against cancer cells is one of the primary objectives for effective cancer treatment. Natural alkaloids of *Chelidonium majus,* have been reported to induce various cell death mechanisms especially through apoptosis induction [15]. The most important benzylisoquinolines in this plant include chelidonine, sangunarine, chelerythrine, and berberine with slightly different structures and various extents of anti-proliferative effects in cancer cell lines [51-54]. However, more investigation is required to elucidate the detailed mechanisms and structure-function relationship relevant to their antiproliferative effects.

This study has focused on a comparative study of selective binding to G4 DNA and anti-telomerase activity of the main alkaloids of *C*. *majus*. MTT experiments revealed that all the compounds were cytotoxic in MCF-7 cells. Chelerythrine and sanguinarine were the most cytotoxic alkaloids, while chelidonine having a hydroxyl group exhibited a relatively less cytotoxicity. Papaverine, a benzyl-isoquinoline alkaloid with fewer aromatic rings in its structure and more flexible than berberine, has shown least cytotoxicity (LD_{50} about 120 μM estimated using MTT). Papaverine also has inhibitory effects on telomerase activity and hTERT expression in both MCF-7 [48] and HepG2 [49].

Detection of telomerase activity using a Quantitative TRAP assay revealed a very low-level of telomerase activity in MCF-7 cells treated with chelidonine or sanguinarine. As this assay

measured the enzyme activity in equal amounts of total protein in samples, the reduced activity implies depletion of the relative amount of the active ribonucleoprotein. Telomerase regulation albeit very complicated, is mainly through transcriptional regulation of the catalytic subunit of the enzyme [53]. In the treated MCF-7 cells with chelidonine and sanguinarine, hTERT mRNA levels followed the same diminution as the telomerase activity. Sub-micromolar concentrations of both chelidonine and sanguinarine led to a significant decrease in telomerase activity along with a decrease in hTERT transcription level. Chelerythrine inhibited telomerase by most extent to ~57% of un-treated control cells at its LD_{50} (2.5 μM). Remarkably, berberine showed a significant decrease in telomerase activity to ~16% of untreated cells at 3 μM concentration. It is noteworthy that, in spite of berberine, which is a potent genotoxin and strong DNA intercalator [54-56], no genotoxicity and hepatotoxicity of chelerythrine and sanguinarine has been suggested in animal model up to 5 mg per 1 kg body weight [2, 57].

Another possible mechanism of telomerase inhibition by small molecules is substrate sequestering through G4 stabilization [58, 59]. Our thermal FRET analysis suggests chelerythrine exhibited greatest affinity and specificity among the studied benzophenantridines towards telomeric G4 DNA (Figure 5). It interacted strongly with the synthetic substrate of telomerase and stabilized the folded G4 structure making it inaccessible to the enzyme. G4 structure stabilization was recorded for sanguinarine in a considerably stronger extent than berberine. The ΔT_m of F21T varied considerably in presence of these three alkaloids, although molecular modeling methods suggest almost the similar mode of interactions and comparable binding energies in the hybrid 3+1 topology [64]. Non-electrostatic interactions in the binding of small molecules to G4 are preferable for telomerase inhibition under physiological conditions [60]. Amongst the alkaloids tested here, chelidonine is estimated to have less non-electrostatic interactions than the others as it has an extra hydroxyl group and lesser number of aromatic rings. As thermal FRET analysis did not detect any considerable increase in melting temperature of F21T in presence of chelidonine, direct interference with the telomerase activity by substrate sequestration may not contribute to the inhibition mechanism. In our ligand-TRAP analysis also, no significant change in telomerase and/or Taq polymerase activity was seen after various incubation times with chelidonine. This is consistent with other reports indicating only a minor DNA binding capacity for chelidonine [51]. In conclusion, chelidonine does not interact with telomerase (after ligand-TRAP data) nor does it

sequester its substrate (after thermal FRET data), but strongly inhibited telomerase mainly through hTERT suppression (after qPCR measurments of the hTERT mRNA). Similarly and in agreement with our previous reports [28, 49], papaverine also showed no significant interaction with telomeric quadruplex.

CD experiments confirm the hybrid 3+1 topology of the G4 structures in presence of the studied alkaloids. The ligands showed no considerable changes to enhance the 260 nm peak, while reduced the negative peak at 234 nm. This implies almost a similar mode of interaction of the ligands with F21T and the unlabeled telo-21G.

In conclusion, chelerythrine, sanguinarine and berberine, interfered with telomerase activity by limiting substrate accessibility; while down-regulation of the hTERT gene may also have an important contribution [61]. It is known that several G-rich regions exist in promoter of hTERT [62]. Whether the latter effect is a consequence of G4 interaction with these isoquinolines requires further investigation. These regions are expected to be additional targets for G4 formation in the presence of chelerythrine, sanguinarine and berberine.

Based on thermal FRET observations, the number of fused aromatic rings of the ligands may have the highest impact on the strength of interaction with telomeric quadruplex. So that by reducing the number of the aromatic rings or separating them a smaller ΔT_m will be expected. Inclusion of polar substitutions may decrease the interaction. The benzophenanthridine alkaloids have stronger interaction with telomeric G4 structure than other isoquinolines. Also, opening the methylene dioxy rings may enhance the interactions. This highlights the priority of aromatic and hydrophobic interactions in binding of these ligands to telomeric G-quadruplex.

Acknowledgments

This work was supported by the Iran National Science Foundation (INSF) granted to S.K.N. J.S. acknowledges support by Praemium Academiae, Czech Republic. JS and BI acknowledge support from the Czech Science Foundation (Grant No 16-13721S) and the CEITEC 2020 project (LQ1601) with financial support from the Ministry of Education, Youth and Sports of the Czech Republic under the National Sustainability

Programme II. S.H. would like to thank the UCL School of Pharmacy for the award of a UCL Excellence Fellowship.

Conflicts of Interest

The authors declare that they have no conflict of interests.

References

1. Amin AR, Karpowicz PA, Carey TE, Arbiser J, Nahta R, Chen ZG, Dong JT, Kucuk O, Khan GN, Huang GS, Mi S, Lee HY, Reichrath J, Honoki K, Georgakilas AG, Amedei A, Amin A, Helferich B, Boosani CS, Ciriolo MR, Chen S, Mohammed SI, Azmi AS, Keith WN, Bhakta D, Halicka D, Niccolai E, Fujii H, Aquilano K, Ashraf SS, Nowsheen S, Yang X, Bilsland A, Shin DM. Evasion of anti-growth signaling: A key step in tumorigenesis and potential target for treatment and prophylaxis by natural compounds. Semin. Cancer Biol. 35 (2015) Suppl: S55-77.

2. Franceschin M, Rossetti L, D'Ambrosio A, Schirripa S, Bianco A, Ortaggi G, Savino M, Schultes C, Neidle S. Natural and synthetic G-quadruplex interactive berberine derivatives. Bioorg Med Chem Lett. 16 (2006) 1707-11.

3. Macha MA, Krishn SR, Jahan R, Banerjee K, Batra SK, Jain M. Emerging potential of natural products for targeting mucins for therapy against inflammation and cancer. Cancer Treat Rev. 41 (2015) 277-288.

4. Ghosh S, Pradhan SK, Kar A, Chowdhury S, Dasgupta D. Molecular basis of recognition of quadruplexes human telomere and c-myc promoter by the putative anticancer agent sanguinarine. Biochim Biophys Acta. 1830(2013) 4189-201.

5. Capistrano IR, Wouters A, Lardon F, Gravekamp C, Apers S, Pieters L. In vitro and in vivo investigations on the antitumour activity of *Chelidonium majus*. Phytomed. 22 (2015) 1279-87.

6. Kim DJ, Ahn B , Han BS, Tsuda H. Potential preventive effects of *Chelidonium majus* L. (Papaveraceae) herb extract on glandular stomach tumor development in rats treated with N-methyl-N'-nitro-N nitrosoguanidine (MNNG) and hypertonic sodium chloride. Cancer Lett. 112 (1997) 203–208.

7. Lohninger A, Hamler F. Chelidonium majus L. (Ukrain) in the treatment of cancer patients. Drugs Exp. Clin. Res. 18 (1992) Suppl:73–77.

8. Gilca M, Gaman L, Panait E, Stoian I, Atanasiu A. *Chelidonium majus* – an Integrative Review: Traditional Knowledge versus Modern Findings. Forsch Komplementmed. 17 (2010) 241–248.

9. Colombo ML, Bosisio E. Pharmacological activities of *Chelidonium majus* L. (Papaveraceae). Pharmacol. Res. 33 (1996) 127–34.

10. Habermehl D, Kammerer B, Handrick R, Eldh T, Gruber C, Cordes N. Proapoptotic activity of Ukrain is based on *Chelidonium majus* L. alkaloids and mediated via a mitochondrial death pathway. BMC Cancer. 6 (2006) 14.

11. Huh J, Liepins A, Zielonka J, Andrekopoulos, Kalyanaraman B, Sorokin A. Cyclooxygenase 2 rescues LNCaP prostate cancer cells from sanguinarine-induced apoptosis by a mechanism involving inhibition of nitric oxide synthase activity. Cancer Res. 66 (2006) 3726–3736.

12. Patil JB, Kim J, Jayaprakasha GK. Berberine induces apoptosis in breast cancer cells (MCF-7) through mitochondrial-dependent pathway. Eur J Pharmacol. 645 (2010) 70-8.

13. Noureini SK, Wink M. Transcriptional down regulation of hTERT and senescence induction in HepG2 cells by chelidonine. World J. Gastroenterol. 15 (2009) 3603-10.

14. Kazemi Noureini S., Esmaili H. Multiple mechanisms of cell death induced by chelidonine in MCF-7 breast cancer cell line. Chem. Biol. Interact. 223 (2014) 141–149.

15. Philchenkov A, Kaminsky V, Zavelevich M, Stoika R. Apoptogenic activity of two benzophenanthrid-ine alkaloids form *Chelidonium majus* L. does not correlate with their DNA damaging effects. Toxicol. In Vitro 22 (2008) 287–295.

16. Cordes N, Plasswilm L, Bamberg M, Rodemann HP. Ukrain, An alkaloid thiophosphoric acid derivative of *Chelidonium majus* L. protects human fibroblasts but not human tumor cells in vitro against ionizing radiation. Int. J. Rad. Biol. 78 (2002) 17–27.

17. Hohenwarter O, Strutzenberger K, Katinger H, Liepins A, Nowicky JW. Selective inhibition of in vitro cell growth by the antitumor drug Ukrain. Drugs Exp. Clin. Res. 18(suppl) (1992) 1–4.

18. Huffman KE, Levene SD, Tesmer VM, Shay JW, Wright WE. Telomere shortening is proportional to the size of the G-rich telomeric 3'-overhang. J. Biol. Chem. 275 (2000) 19719-22.

19. Avilion AA, Piatyszek MA, Gupta J, Shay JW, Bacchetti S, Greider CW. Human telomerase RNA and telomerase activity in immortal cell lines and tumor tissues Cancer Res. 56 (1996) 645-50.

20. Hiyama E, Yokoyama T, Tatsumoto N, Hiyama K, Imamura Y, Murakami Y. Telomerase activity in gastric cancer. Cancer Res. 55 (1995) 3258-3262.

21. Smith LL, Coller HA, Roberts JM. Telomerase modulates expression of growth-controlling genes and enhances cell proliferation. Nat. Cell Biol 5 (2003) 474-479.

22. Stewart SA, Weinberg RA. Telomeres: cancer to human aging. Ann. Rev. Cell Dev. Biol. 22 (2006) 531–557.

23. Hwang H, Kreig A, Calvert J, Lormand J, Kwon Y, Daley JM, Sung P, Opresko PL, Myong S. Telomeric overhang length determines structural dynamics and accessibility to telomerase and ALT-associated proteins. Structure. 22 (2014) 842-53.

24. Maji B, Bhattacharya S. Advances in the molecular design of potential anticancer agents via targeting of human telomeric DNA. Chem Commun (Camb). 50 (2014) 6422-38.

25. Joseph I, Tressler R, Bassett E, Harley C, Buseman CM, Pattamatta P, et al. The telomerase inhibitor imetelstat depletes cancer stem cells in breast and pancreatic cancer cell lines. Cancer Res. 70 (2010) 9494-504.

26. Crees Z, Girard J, Rios Z, Botting GM, Harrington K, Shearrow C, Wojdyla L, Stone AL, Uppada SB, Devito JT, Puri N. Oligonucleotides and G-quadruplex stabilizers: targeting telomeres and telomerase in cancer therapy. Curr Pharm Des. 20 (2014) 6422-37.

27. Schultes CM, Guyen B, Cuesta J, Neidle S. Synthesis, biophysical and biological evaluation of 3,6-bis-amidoacridines with extended 9-anilino substituentsas potent G-quadruplex-binding telomerase inhibitors. Bioorg Med Chem Lett. 14(2004) 4347-51.

28. Abachi F, Kazemi Noureini S. Evaluation of natural compounds for telomeric DNA interaction using FRET thermal melting analysis. Clin. Biochem. 44 (2011) 13, S257.

29. Bessi I, Bazzicalupi C, Richter C, Jonker HR, Saxena K, Sissi C, Chioccioli M, Bianco S, Bilia AR, Schwalbe H, Gratteri P.Spectroscopic, molecular modeling, and NMR-spectroscopic investigation of the binding mode of the naturalalkaloids berberine and sanguinarine to human telomeric G-quadruplex DNA. ACS Chem Biol. 7(2012) 1109-19.

30. Bhadra K, Maiti M, Kumar GS.DNA-binding cytotoxic alkaloids: comparative study of the energetics of binding of berberine, palmatine, andcoralyne. DNA Cell Biol. 27 (2008) 675-85.

31. Bessi I,Bazzicalupi C, Richter C, Jonker HR, Saxena K, Sissi C, Chioccioli M, Bianco S, Bilia AR, Schwalbe H, Gratteri P. Spectroscopic, Molecular Modeling, and NMR-Spectroscopic Investigation of the Binding Mode of the Natural Alkaloids Berberine and Sanguinarine to Human Telomeric G-Quadruplex DNA. ACS Chem Biol. 7 (2012) 1109-19.

32. Mosmann T. Rapid colorimetric assay for cellular growth and survival; application to proliferation and cytotoxicity assays. J Immunol Methods. 65 (1983) 55-63.

33. Kim NW, Piatyszek MA, Prowse KR, Harley CB, West MD, Ho PL. Specific association of human telomerase activity with immortal cells and cancer. Science. 266 (1994) 2011-50.

34. Bradford MM. A rapid and sensitivi method for quantific).For each of control and/in utilizing the principle of protein-dye binding. Anal Biochem. 72 (1976) 248-254.

35. Hou M, Dawei X, Byorkltolm M, Gruber A. Real-Time quantitative telomeric repeat amplitication protocol Assay for the detection of telomerase activity. Clin Chemistry. 47 (2001) 519-24.

36. Noureini SK, Wink M. Antiproliferative effects of crocin in HepG2 cells by telomerase inhibition and hTERT down-regulation. Asian Pac. J. Cancer Prev. 13 (2012) 2305-9.

37. Kazemi Noureini S, Tanavar F. Boldine, a natural aporphine alkaloid, inhibits telomerase at non-toxic concentrations. Chem. Biol. Interact. 231 (2015) 27-34.

38. Guédin A, Lacroix L, MergnyJL. Thermal Melting Studies of Ligand DNA Interactions Drug-DNA Interaction Protocols. Methods Mol. Biol. 613 (2010) 25-35.

39. Ohnmacht SA, Neidle S. Small-molecule quadruplex-targeted drug discovery. Bioorg Med Chem Lett. 24 (2014) 2602–2612.

40. Katritch, V., Totrov, M. & Abagyan, R. ICFF: a new method to incorporate implicit flexibility into an internal coordinate force field. J. Comp. Chem. 24 (2003) 254-265.

41. Case DA, Berryman JT, Betz RM, Cerutti DS, Cheatham TE, Darden TA, Duke RE, Giese TJ, Gohlke H, Goetz AW, Homeyer N, Izadi S, Janowski P, Kaus J, Kovalenko A, Lee TS, LeGrand T, Li P, Luchko T, Luo R, Madej B, Merz KM, Monard G, Needham P, Nguyen H, Nguyen HT, Omelyan I, Onufriev A, Roe DR, Roitberg A, Salomon-Ferrer R, Simmerling CL, Smith W, Swails J, Walker RC, Wang J, Wolf RM, Wu X, York DM and Kollman PA (2015), AMBER 2015, University of California, San Francisco.

42. Perez, A. Marchán I, Svozil D, Sponer J, Cheatham TE 3rd, Laughton CA, Orozco M. Refinement of the AMBER force field for nucleic acids: improving the description of alpha/gamma conformers. Biophys. J. 92 (2007) 3817–3829.

43. Krepl, M. Zgarbová M, Stadlbauer P, Otyepka M, Banáš P, Koča J, Cheatham TE 3rd, Jurečka P, Sponer J. Reference simulations of noncanonical nucleic acids with different chi variants of the AMBER force field: quadruplex DNA, quadruplex RNA and Z-DNA. J. Chem. Theory Comput. 8 (2012) 2506–2520.

44. Cornell WD, Cieplak P, Bayly CI, Gould IR, Merz KM, Ferguson DM, Spellmeyer DC, Fox T, Caldwell JW, Kollman PA. A 2nd generation force-field for the simulation of proteins, nucleic acids and organic-molecules. J. Amer. Chem. Soc. 117 (1995) 5179–5197.

45. Joung IS and Cheatham TE Determination of Alkali and Halide Monovalent Ion Parameters for Use in Explicitly Solvated Biomolecular Simulations. J. Phys. Chem. B112 (2008) 9020–9041.

46. Harvey, MJ, Giupponi G, and Fabritiis GD, ACEMD: Accelerating Biomolecular Dynamics in the Microsecond Time Scale. J. Chem. Theo. Comp. 5 (2009) 1632-1639

47. Humphrey W, Dalke A and Schulten K, VMD: Visual molecular dynamics. J. Mol. Graphics. 14 (1996) 33-38.

48. Noori ZS., Kazemi Noureini S., Nabiuni M. Investigation of Telomerase activity and hTERT gene expression in MCF7 cells treated with papaverine. Journal of Sabzevar University of Medical Sciences. 20 (2013) 122-132.

49. Kazemi Noureini S., Wink M. Antiproliferative Effect of the Isoquinoline Alkaloid Papaverine in Hepatocarcinoma HepG-2 Cells — Inhibition of Telomerase and Induction of Senescence Molecules. 19 (2014) 11846-59.

50. De Rache A, Mergny JL. Assessment of selectivity of G-quadruplex ligands via an optimized FRET melting assay. Biochimie. 115 (2015) 194-202.

51. Kaminskyy V, Zavelevich M, Stoika R. Apoptogenic activity of two benzophenanthridine alkaloids from Chelidonium majus L. does not correlate with their DNA damaging effects. Toxicol. In Vitro. 22 (2008) 287-95.

52. Lu JJ, Bao JL, Chen XP, Huang M, Wang YT. Alkaloids Isolated from Natural Herbs as the Anticancer Agents. Evid Based Complement Alternat Med 2012 (2012) 485042.

53. Counter CM, Meyerson M, Eaton EN, Ellisen LW, Caddle SD, Haber DA. Telomerase activity is restored in human cells by ectopic expression of hTERT (hEST2), the catalytic subunit of telomerase. Oncogene. 16 (1998) 1217–1222.

54. Pasqual MS, Lauer CP, Moyna P, Henriques JA. Genotoxicity of the isoquinoline alkaloid berberine in prokaryotic and eukaryotic organisms. Mutat. Res. 286 (1993) 243-52.

55. Wang Y, Liu Q, Liu Z, Li B, Sun Z, Zhou H, Zhang X, Gong Y, Shao C. Berberine, a genotoxic alkaloid, induces ATM-Chk1 mediated G2 arrest in prostate cancer cells. Mutat Res. 734 (2012) 20-29.

56. Kosina P, Walterová D, Ulrichová J, Lichnovský V, Stiborová M, Rýdlová H, Vičar J, Krečman V, Brabec MJ, Šimánek V. Sanguinarine and chelerythrine: assessment of safety on pigs in ninety days feeding experiment. Food Chem. Toxicol. 42 (2004) 85–91.

57. Berardinelli F, Siteni S, Tanzarella C, Stevens MF, Sgura A, Antoccia A. The G-quadruplex-stabilising agent RHPS4 induces telomeric dysfunction and enhances radiosensitivity in glioblastoma cells. DNA Repair. 25 (2015) 104–115.

58. Salem AA, El Haty IA, Abdou IM, Mu Y. Interaction of human telomeric G-quadruplex DNA with thymoquinone. A possible mechanism for thymoquinone anticancer effect. Biochim Biophys Acta. 1850 (2015) 329–342.

59. Nielsen MC, Larsen AF, Abdikadir FH, Ulven T. Phenanthroline-2,9-bistriazoles as selective G-quadruplex ligands. Eur. J. Med. Chem. 72 (2014) 119–126.

60. Xiong Y-X, Huang Z-H, Tan J-H. Targeting G-quadruplex nucleic acids with heterocyclic alkaloids and their derivatives. Eur J Med Chem. 7 (2015) 538-551.

61. Yaku H, Murashima T, Tateishi-Karimata H, Nakano S, Miyoshi D, Naoki Sugimoto N. Study on effects of molecular crowding on G-quadruplex-ligand binding and ligand-mediated telomerase inhibition. Methods. 64 (2013) 19-27.

62. Lim KW, Lacroix L, Yue DJ, Lim JK, Lim JM, Phan AT. Coexistence of two distinct G-quadruplex conformations in the hTERT promoter. J Am Chem Soc. 132 (2010) 12331-42.

63. Parkinson GN, Lee MP, Neidle S. Crystal structure of parallel quadruplexes from human telomeric DNA. Nature. 417 (2002) 876-80.

64. Chung WJ, Heddi B, Tera M, Iida K, Nagasawa K and Phan AT. Solution structure of an intramolecular (3+1) human telomeric g-quadruplex bound to a telomestatin derivative. J. Am. Chem. Soc. 135 (2013) 13495-13501

65. Zhou J, Fleming A, Averill A, Burrows C and Wallace SS. The NEIL glycosylases remove oxidized guanine lsions from telomeric and promoter quadruplex DNA structures. Nucleic Acids Res. 43 (2015) 8:4039-4054

Figure Legends

Figure 1: Chemical structures of berberine, chelidonine, chelerythrine, sanguinarine, and papaverine.

Figure 2: Cell viability of MCF7 cells after 24 (light gray), 48 (gray) and 72 (black) hours treatment with different concentrations of berberine, chelerythrine, chelidonine and sanguinarine as estimated by MTT. Mean values ± standard error of means is shown.

Figure 3: CD spectra of telo-21G at 1 μM concentration in 10 mM sodium cacodylate buffer and 100 mM KCl pH 7.2 alone (purple) and in the presence of an increasing ligand concentration of chelerythrine, sanguinarine, berberine, chelidonine and papaverine represented by green, black, red, blue, yellow curves respectively at ratios 1:1 (A), 10:1 (B), 100:1 (C) (ligand/ telo-21G. (D) Chelerythrine in the presence of telo-21G at 0.25 and 0.5 μM (2:1, 4:1) in light green, and dark green lines respectively.

Figure 4: Telomerase activity (grey line) and hTERT mRNA level (black line) estimated using q-TRAP and real-time PCR in MCF-7 cells after 48h treatment with the alkaloids. The mean value ± SEM of four logical repeats, each including at least three samples for different concentrations has been presented.

Figure 5A: **Top:** Classical thermal FRET analysis of F21T in 10mM sodium cacodylate, pH 7.2 and 100 mM K+ alone (black) or equimolar concentration of **Ber**berine (dark blue), **Che**lidonine (red), **Ch**ele**r**ythrine (green), **Pap**averine (blue) and **San**guinarine (orange). **Middle:** t-FRET melting measurements of F21T in the same buffer mentioned above and presence of equimolar concerntation of the complementary oligonucleotide CT22. Its shows two tandem sigmoid curves starting with high fluorescence intensity at the beginning of FRET measurements where F21T:CT22 may form double stranded duplex DNA followed by a clear transition step, marked as "a". By increasing temperature F21T will be released and may fold into G4 structure (GQ). By continuing heating, a second transition step occurs due to denaturation of the quadruplexes, marked as "b", until the G-rich strand is also completely unfolded. **Bottom:** tFRET melting measurements of F21T in 10mM sodium cacodylate, pH 7.2 and 100 mM KCl in presence of

equimolar concentration of the complementary oligonucleotide CT22 and 1:1 concentration ratio of alkaloids as above. Note the similar pattern of this second sigmoidal (boxed rectangle) with the classic FRET melting curve illustrated above.

Figure 5B: (**Left**) Classical FRET melting of 0.25 μM F21T (black) in 10mM sodium cacodylate, pH 7.2 and 100 mM KCl alone (blue) or in presence of 1:1 (red) , 10:1 (green) and 100:1 (purple) ratios of berberine, chelerythrine, chelidonine, papaverine and sanguinarine. (**Middle**) Transition FRET (tFRET) melting analysis of equimolar concentration of F21T and CT22 (0.25 μM each) in 10 mM and 100mM sodium cacodylate without any alkaloid (black) or in presence of 1:1 (red) , 10:1 (green) and 100:1 (violet) ratios of berberine, chelerythrine, chelidonine, papaverine and sanguinarine. (**Right**) Classical thermal $CD_{290\ nm}$ melt analysis of telo-21G at 1 μM in 10 mM sodium cacodylate and 100 mM KCl in presence of final concentrations of 0, 1, 10, and 100 μM ligands (0:1, 1:1,10:1, 100:1 ligand/ telo-21G) in blue, red, green, purple lines respectively.

Figure 6: (A) The difference in $T_{1/2}$ of telo-21G in $CD_{290\ nm}$ melting test and (B) F21T in classical FRET melting in sodium cacodylate buffer, pH 7.2 and 100 mM KCl and in presence of increasing concentrations of alkaloids.

Figure 7: Conformations of the alkaloids when bound to 3+1 hybrid topology G4 DNA [64]. The central nitrogen in Chelerythrine (green), berberine (yellow), chelidonine (black), sanguinarine (red) and papaverine (blue) orients on top of the electronegative channel in the quadruplex structure. The side view of how all ligands bind is illustrated in the bottom right corner.

Figure 8: Ligand-TRAP measurements. A master mix of q-TRAP reaction including MCF-7 cell lysate was prepared and aliquoted to two sets on ice. Various concentrations of the desired alkaloid berberine, chelerythrine and sanguinarine were added as explained in part 2.3. Treatments in 1, 3 and 5 have been done before primer elongation by telomerase and in 2, 4 and 6 before q-PCR. In samples 1, 3 and 5 both telomerase and hot-start Taq polymerase have been exposed to the alkaloids while in samples 2, 4 and 6 only hot-start Taq enzyme has been exposed to the alkaloids.

Selectivity of major isoquinoline alkaloids from *Chelidomium majus* towards telomeric G-quadruplex: A study using a modified transition-FRET (t-FRET) assay.

Sakineh Kazemi Noureini[a,*], Hosein Esmaeili[a], Farzane Abachi[a], Soraia Khiali[f], Barira Islam[b], Martyna Kuta[d], Ali A. Saboury[e], Marcin Hoffmann[d], Jiri Sponer[b,c], Gary Parkinson[f], Shozeb Haider[f,*]

[a] Deptartment of Biology, Faculty of Basic Sciences, Hakim Sabzevari University, P.O.Box: 397, Sabzevar, Iran
[b] Institute of Biophysics, Academy of Sciences of the Czech Republic, Královopolská 135, 612 65 Brno, Czech Republic
[c] Central European Institute of Technology (CEITEC), Masaryk University, Campus Bohunice, Brno, Czech Republic
[d] Adam Mickiewicz University, Poznan, Poland
[e] Institute of Biochemistry and Biophysics, University of Tehran, Tehran, Iran
[f] UCL School of Pharmacy, Brunswick Square, London, UK

*** Corresponding Authors:**
Sakineh Kazemi Noureini
Deptartment of Biology, Faculty of Basic Sciences, Hakim Sabzevari University,
P.O.Box: 397, Sabzevar, Iran
Email: kazemibio@gmail.com
Tel.: +98-5144013012
Fax: +98-5144013365.

And

Shozeb Haider
UCL School of Pharmacy
29-39 Brunswick Square
London WC1N 1AX
UK
Email: Shozeb.haider@ucl.ac.uk
Tel.: +44-2077535883

Structured Abstract

Background

Natural bioproducts are invaluable resources in drug discovery. Isoquinoline alkaloids of *Chelidonium majus* constitute a structurally diverse family of natural products that are of great interest, one of them being their selectivity for human telomeric G-quadruplex structure and telomerase inhibition.

Methods

The study focuses on the mechanism of telomerase inhibition by stabilization of telomeric G-quadruplex structures by berberine, chelerythrine, chelidonine, sanguinarine and papaverine. Telomerase activity and mRNA levels of hTERT were estimated using quantitative telomere repeat amplification protocol and qPCR, in MCF-7 cells treated with different groups of alkaloids. The selectivity of the main isoquinoline alkaloids of *Chelidonium majus* towards telomeric G-quadruplex forming sequences were explored using a sensitive modified thermal FRET-melting measurement in the presence of the complementary oligonucleotide CT22. We assessed and monitored G-quadruplex topologies using circular dichroism (CD) methods, and compared spectra to previously well-characterized motifs, either alone or in the presence of the alkaloids, Molecular modeling was performed to rationalize ligand binding to the G-quadruplex structure.

Results

The results highlight strong inhibitory effects of chelerythrine, sanguinarine and berberine on telomerase activity, most likely through substrate sequestration. These isoquinoline alkaloids interacted strongly with telomeric sequence G-quadruplex. In comparison, chelidonine and papaverine had no significant interaction with the telomeric quadruplex, while they strongly inhibited telomerase at transcription level of hTERT. Altogether, all of the studied alkaloids showed various levels and mechanisms of telomerase inhibition.

Conclusions

We report on a comparative study of anti-telomerase activity of the isoquinoline alkaloids of *Chelidonium majus*. Chelerythrine was most effective in inhibiting telomerase activity by substrate sequesteration through G-quadruplex stabilization.

General Significance

Understanding structural and molecular mechanisms of anti-cancer agents can help in developing new and more potent drugs with fewer side effects. Isoquinolines are the most biologically active agents from *Chelidonium majus*, which have shown to be telomeric G-quadruplex stabilizers and potent telomerase inhibitors.

Keywords: chelerythrine, sanguinarine, berberine, chelidonine, papaverine telomerase, t-FRET, transition, G-quadruplex

Highlights:

- Isoquinoline alkaloids from *Chelidonium majus* bind selectively to telomeric G-quadruplex and inhibit telomerase activity via substrate sequestration
- Selectivity to G-quadruplex studied using a novel, sensitive modified transition-FRET (tFRET) assay in the presence of complimentary oligonucleotide
- The ligands bind to the terminal quartet and maximize π-π stacking interactions in the 3+1 hybrid topology quadruplex

1. Introduction

Bioactive natural compounds have been explored as new agents to combat malignancies, overcome drug-resistance and prevent carcinogenesis [1]. Telomerase is a key target for therapeutic intervention in cancer cells. It has been shown to be selectively inhibited by natural products including berberine, sanguinarine and their derivatives via G-quadruplex (G4) stabilization [2,3]. The extract and derivatives from *Chelidonium majus* have been used in treatment of several malignancies including gastric and breast cancer since 1896 [4-7]. The extract includes several chemically and pharmacologically interesting alkaloids [8], in which the most biologically active components are isoquinolines and their derivatives (Figure 1) [9]. Isoquinolines have shown different cytotoxic mechanisms in several transformed and malignant cell types [9-14]. For example, chelidonine and sanguinarine have shown varying apoptogenic strength without DNA damage [15], while some others have shown radio-protective effects on normal but not cancer cells [16]. Ukarin, a synthetic derivative related to these compounds, has shown selective inhibition of cancer cells, with no significant toxicity in normal cells even at much higher concentrations [17]. Of the several mechanisms, inhibition of telomerase via G4 stabilization remains an attractive proposition.

The enzyme telomerase is over-expressed, by up to a hundred-fold, in more than 85% of cancer cells [18]. It rescues cancer cells from end-replication problem by maintaining telomere length using its intrinsic RNA as the template [19], thus conferring a strong selective advantage for continued growth of malignant cells [20-22]. The guanine-rich, single strand terminal ends of telomeres may fold into a strong and stable intramolecular G4 structures, which prevents accessibility to telomerase [23]. Various strategies have targeted this structure to suppress telomerase activity in rapidly dividing cancer cells [24-26].

One approach put forward by the Neidle group is to stabilize G4 structures using small molecules; thereby preventing access to single stranded telomeric DNA for telomere elongation by telomerase [27]. Our previous screening studies on G4 stabilizing natural agents showed that isoquinoline alkaloids of *Chelidonium majus* could suppress proliferation and active telomerase content of cancer cells [13, 14, 28]. Various sets of isoquinolines like berberine have been studied for their mode of interactions with telomeric G4 DNA including their stoichiometry [29] and energetics of binding [30]. Molecular modeling and NMR spectroscopic data are available on berberine and

sanguinarine, highlighting their selectivity for G4 DNA and the dominant role aromatic moieties play in G4 binding [2,31].

In this study, we focused our investigation on the mechanisms of telomerase inhibition by stabilizing G4 DNA via berberine, chelerythrine, chelidonine, sanguinarine and papaverine. We explored hTERT expression level in parallel with telomerase activity in treated cells. The probable direct interaction of the compounds with telomerase ribonucleoprotein were studied using ligand-TRAP experiments and the selectivity of ligand binding to telomeric G4 DNA versus ds-DNA was explained by classical and a novel modified thermal FRET-melting assays. Sequence dependence G4 topology, associated ligand preference and thermal stability to various alkaloids was also monitored using CD methods.

2. Material and methods

2.1. Cell culture and cytotoxicity

Human breast adenocarcinoma cell line MCF7 (ACC115 from DSMZ) were maintained in 75 cm^2 culture flasks in DMEM, supplemented with 10% heat-inactivated fetal bovine serum, 100 U/ml penicillin, and 100 µg/ml streptomycin (all the materials from PAA, Austria). Cells were grown in 5% CO_2 and 90% humidity at 37°C. Cell viability was evaluated routinely by trypan blue exclusion method using a hemocytometer.

Among the commercially available different classes of isoquinoline alkaloids, 12 pure compounds were purchased from Sigma-Aldrich. Cytotoxicity of the compounds was estimated using MTT method [32]. Briefly, cells in the exponential phase (24 hours after seeding in 96 well plates 10000 cells per well) were incubated with various concentrations of the desired compound freshly prepared from the stock solutions (10 or 50 mM in absolute ethanol). The final concentration of ethanol was always less than 0.1%. After incubation for 48 hours, MTT 3-(4,5-dimethylthiazol-2-yl)-2,5-diphenyl-tetrazolium bromide (Sigma-Aldrich) was added to a final concentration of 0.5 mg/ml to each well. The plate was further incubated for four hours for MTT reduction to formazan purple product through mitochondrial dehydrogenases of viable cells. The absorbance was read at 570 nm using a plate reader (BioTek, USA) after dissolving the formazan product in dimethylsulfoxide containing 10% SDS and 1% acetic acid. The tests were repeated at least 3 times each in triplicates and the LD_{50} values were calculated from dose-response curves using Gen5 version1.06 software.

2.2. Circular dichroism

The oligonucleotide telo-G21 (5'-GGG(TTAGGG)$_3$-3') was purchased from Eurofins Genomics. The sample was first dissolved in water, then diluted to a final concentration of 0.01 mM in buffer consisting of KCl (100 mM) and sodium Cacodylate (10 mM, pH 7.2). The sample was heated at 95°C in the heating block for two minutes and then left cooling overnight at room temperature and then stored at 4°C. The ligands, chelerythrine, papaverine, berberine and chelidonine, were purchased from Sigma-Aldrich, the sanguinarine was purchased from Cambridge bioscience. They were all dissolved in di-methyl sulfoxide (DMSO) at the final concentration of 33 mM and then

stock solutions of ligands at the concentrations of 0.01 mM, 0.1 mM and 1 mM were prepared doing several dilutions with water.

Twenty solutions (final volume 0.2 ml) of complexes DNA-ligands were prepared adding DNA solution (final concentration 0.001 mM), in sodium Cacodylate buffer (final concentration 10 mM, pH 7.2 and KCl 100 mM), water to take to volume and the right amount of ligand solution to obtain the final concentrations of 1 mM, 0.1 mM, 0.01 mM and 0.001 mM for each ligand, and two more solutions of complex DNA-chelerythine were prepared at these ratios: 1:4 and 1:2. The solutions were incubated at 37°C for two hours, then circular dichiroism experiments were carried out on Chirascan Plus using quartz cells of 0.1 cm path length (scan rate 4 s/nm) at 25°C.

2.3. Quantitative Telomere Repeat Amplification Protocol (q-TRAP)

Sub-confluent MCF-7 cells were seeded in 6 well plates and incubated for 48 hours with various concentrations of the test compound. Cells were washed with PBS, lysed according to Kim *et al*. [33] and incubated for 30 min at 4°C. The lysates were centrifuged at 16,000×g for 30 min at 4°C. Protein concentration of supernatant was measured by Bradford method [34]. Q-TRAP assay was performed by real-time SYBR-Green method [35] with small modifications as previously reported [36]. The reaction mixtures including 1X SYBR Green master mix (GenetBio, South Korea), 1 µg protein of cell extract, 10 pmol TS (5'-AATCCGTCGAGCAGATT-3') and 5 pmol ACX (5'-GCGCGGCTTACCCTTACCCTTACCCTAACC-3') primers were incubated for 30 min at 25°C. DNA products from telomerase activity were amplified using the following conditions: The hot-start taq polymerase was activated by heating at 94°C for 10 min followed by 40 cycles of 30 sec at 94°C, 30 sec at 50°C and 45 sec at 72°C with signal acquisition on a real-time thermal cycler Rotor Gene 3000 (Corbett Research). The threshold cycle values (Ct) determined by Rotor Gene 6.01 software were compared with the standard curve generated from serially diluted cell lysate of untreated MCF-7 control. Each experiment included a negative control, which was a reaction mix without cell extract or a heat / RNase-treated sample to inactivate telomerase. This experiment was performed for every test compound in at least three logically independent repeats with three or more samples per point.

For ligand-TRAP tests, the reactions were incubated with the desired concentrations of alkaloid before or after telomerase activity as explained above [37] with small modifications. Briefly, a master mix of q-TRAP reaction including MCF-7 cell lysate was prepared and aliquoted to two sets on ice (A and B). Various concentrations of the desired alkaloid were added to samples of set A and incubated for 30 minutes on ice. Then all samples of both sets were incubated for 20 min at 24°C for extending TS primer by telomerase. All the samples were put back on ice and the same concentrations of alkaloid as set A was added to the samples of set B. Only Taq polymerase will be exposed to the alkaloids in this set. The amplification and quantification were done as described in the previous section. This experiment has been repeated at least three times, and each repeat included triplicate samples for each concentration of the alkaloid. Traces of RNase contamination that potentially can give rise to false positive results was checked by incubating total RNA with aliquots of the alkaloids for 0 or 30 min at room temperature followed by electrophoresis in agarose gel.

2.4. Total RNA isolation, cDNA synthesis and Real-time PCR

Total RNA was isolated from the control and treated MCF-7 cells using RNX-Plus solution (SinaClone BioScience, Iran) according to the manufacturer's instructions. cDNA synthesis was performed on 2 µg of each sample using MMULV reverse transcriptase (Vivantis, Korea). Expression levels of the hTERT and β2 microglubolin genes were detected by quantitative reverse transcription polymerase chain reaction (qRT-PCR) that used specific intron-spanning primers as explained above [36]. Briefly, 1 µl of each cDNA sample was subjected to PCR-amplification reaction including SYBR Green PCR Master Mix (GenetBio, Korea) and 5 pmol of each primer. Relative mRNA copy number of hTERT gene to that of the housekeeping gene, β2 microglubolin, was compared among the control and treated samples using the related standard curves calculated by Rotor-Gene 6.01 software.

2.5. Thermal FRET and CD analysis

The probable interaction of the alkaloids with telomerase substrate and interference with the enzyme activity was estimated through a simple thermal melting experiment based on Guedin *et al*., 2010 [38] with small modifications. By using these methods we can demonstrate the structural stabilization effect of the alkaloids on a dual-labeled fluorescence synthetic oligonucleotide of

human telomere sequence rich in guanine, F21T (FAM 5'-GGG(TTAGGG)$_3$-3' TAMRA) and native telo-21G (5'-GGG(TTAGGG)3-3'), which inherently fold to an intramolecular G4 DNA. Fluorescence intensity of F21T was measured while heating gradually from 30 to 98°C at the rate of 1°C/min while for CD from 37 to 98°C at the rate of 1min/°C. G4 DNA structures unfold at high temperatures. The temperature at which the transition from folded to unfold structure occurs, correlates to the melting temperature (T_m). The ligands that preferentially bind to and stabilize the folded state of F21T and unlabeled telo-21G increase its T_m.

FRET fluorescence intensity increased in an almost two state denaturation pattern. Briefly, F21T at final concentration of 0.25 µM was heated at 95°C for 10 min, immediately chilled on ice and incubated at 37°C for 2 h in presence of sodium cacodylate (10mM) and KCl (100 mM); and equimolar concentration of the desired alkaloid. Fluorescence intensity of F21T was detected using Rotor Gene 3000 real-time thermal cycler (Corbett Research) as the temperature was increased at the rate of 1°C/min. The correlated melting temperatures were calculated by using differential fluorescence intensity of F21T as a function of temperature with Rotor Gene software version 1.06 and compared with that of the oligonucleotide alone. The denaturation pattern monitored by CD shows a single state melt unmodified by the presence of ligands (Figure 5B). For CD thermal experiments the materials were prepared as previously described, where the signals were collected after each step of increasing temperature by the rate of 1°C/min from 37 to 90°C from 220 nm to 320 nm (scan rate 0.5 s/nm).

Another set of FRET experiments, called transition FRET (t-FRET), were conducted with a similar protocol except that the reactions contained equimolar concentrations of the complementary oligonucleotide CT22 (CCCTAA)$_3$CCCT and F21T. After initial heating to unfold the oligonucleotides and immediately chilling on ice, folding to duplex or quadruplex can occur competitively by incubating at 37°C. The duplexes will cause strong fluorescence intensity of F21T due to the greater distance between the dyes in duplex structure relative to quadruplex structure. This set of experiments may evaluate the binding specificity of the compounds to quadruplex structure of F21T with low fluorescence. The higher fluorescence intensity at the start point of FRET measurement demonstrates priority of unfolded state of F21T, which participates in duplex DNA with the CT22 oligonucleotide. However, in presence of ligands, lower fluorescence

intensity at the beginning of the FRET measurement can be explained with folded state of F21T into quadruplex that is stabilized with high affinity of the ligand to this structure. In such cases, the melting temperature is expected to be higher than control samples.

2.6. Molecular Dynamics (MD) simulations

The hybrid 3+1 topology of intramolecular telomeric quadruplex (PDB id 2MB3) was used as the starting point to study G4-ligand interactions [64]. The docking and molecular dynamics protocol was adapted from Ohnmacht et al. [39].

The chemical structures of the ligands were sketched, built and docked using ICM-Pro software [40]. The charges were assigned using the ICFF force field. Grid maps were made that encompassed the terminal quartet. Docking was done using the automated docking module in ICM-Pro software, employing the default parameters. The final docked conformation was chosen based on the strongest binding energy between the docked ligand and the quadruplex. The docked complex for each ligand was chosen as the starting structure for MD simulations.

The stability of ligand-G4 complexes were assessed by MD simulations. The complexes were set up using the xleap module in the AMBER14 molecular dynamics package [41]. The simulations were carried out in parmbsc1 version of Cornell et al. force field with X_{OL4} modifications [42-44]. The system was solvated in a periodic box whose boundaries extended at least 10 Å from any solute atom. The complexes were neutralized by adding K^+ ions and Amber-adapted Joung and Cheatham parameters specific for TIP3P waters were used [45].

The complexes were first minimised using 1000 steps of steepest descent, followed by 1000 steps of conjugate gradient minimisation. A 300 ps of MD equilibration was run in which the G4 was restrained while the ions and water were allowed to equilibrate. The systems were gently heated from 0 K to 300 K with a time step of 0.5 ps followed by another round at constant pressure at 300 K for 1 ns. The constraints were gradually relaxed until no constraints were applied on the systems. The final production MD run was carried out for 250 ns using ACEMD [46]. The default parameters were used and included 10Å non-bonded cut-off,

0.0001Å tolerance was allowed for the SHAKE algorithm, an integration step of 2 fs, constant pressure of 1 ATM at 300 K temperature. The frames were collected every 20 ps and the analysis of the trajectory was performed using the CPPTRAJ module of AMBER. VMD was used to visualise the trajectories [47] and the figures were made in the ICM-Pro software.

2.7. Statistical analysis

Statistical analysis was performed by using one-way ANOVA test and a $p < 0.05$ was considered as the cut off for significant difference.

3. Results

3.1. The alkaloids showed different level of cytotoxicity in cell culture

MTT experiments in 48 h treated MCF-7 cells with berberine, chelidonine, sanguinarine and chelerythrine (Figure 1) estimated LD_{50} values as 54, 8, 3 and 2.5 µM respectively. The cytotoxic effects of all of the compounds are strongly time- and dose-dependent. The rate of cell death increased sharply even at very low concentrations, while it reached a gradual rate around and beyond the LD_{50} (Figure 2). Papaverine was the least cytotoxic compound amongst these alkaloids. Its 48h LD_{50} has been previously reported to about 120 µM in MCF7 [48] and HepG2 cells [49].

3.2. Isoquinoline alkaloids generally do not change the CD signature of telo-21G in annealed in either sodium or potassium.

A positive peak at 251 nm and two small maxima at 271 and 288 nm were seen in the CD spectrum of the human telomeric sequence telo-21G (Figure 3), similar to when annealed in either potassium or sodium buffers (data not shown). The human telomeric sequence may adopt an anti-parallel, parallel, or 3+1 hybrid G-quadruplex topologies. The observed CD spectrum suggests a mixture of G-quadruplex conformations with different proportions or an interchangeable base stacking within the structures [47,65]. However in presence of the ligands the signature remained unchanged except for a slightly stronger intensity of the maxima at 288 nm and a small decrease in maxima at 271 than the telo-21G alone except for chelerythrine. The strongest changes were observed in presence of chelerythrine followed by modest changes for berberine, chelidonine, sanguinarine, and papaverine. Chelerythrine at the molar ratio of 1:4 ligand:telo-21G made as

large as ~12% stronger maxima at 288 and ~16% decrease in minimum at 238 nm than telo-21G alone (Figure 3). A moderate shift about 3.8 and 5.4°C in $T_{1/2}$ of telo-21G in presence of chelerythrine at molar ratio of 1:4 and 1:2 ligand: telo-21G was detected in thermal CD experiment.

3.3. Telomerase activity was suppressed by alkaloids to various extents

Quantitative telomere-repeat amplification protocol (qTRAP) measurements assessed IC_{50} levels of each compound in samples containing equal amounts of total protein (Figure 4). A dose-dependent inhibitory effect was seen in MCF-7 cells treated with the alkaloids. The concentration of the alkaloid that leads to 50% telomerase inhibition in MCF-7 cells after 48 hours incubation, its $IC_{50,}$ was estimated as 27, 1.25, 1, 1.25 and 60 μM for berberine, chelerythrine, chelidonine, sanguinarine and papaverine respectively. In the treated cells berberine at LD_{50} concentration (estimated using MTT assay) suppressed telomerase activity down to 10% of untreated cells. The LD_{50} concentration of chelerythrine showed 60% inhibition of telomerase in the qTRAP assay, although it was able to inhibit telomerase even at a very low concentration in a dose-dependent manner. Telomerase activity was strongly inhibited at very low concentrations of chelidonine or sanguinarine and progressed to almost complete inhibition at their respective LD_{50}.

3.4. Chelidonine decreased hTERT expression significantly

All of the studied alkaloids showed a decreasing effect on the relative hTERT mRNA levels in treated MCF-7 cells (Figure 4, black lines). Berberine, inhibited hTERT transcription down to about 18 ± 5.2% of untreated control cells at 3 μM and with no further decrease up to its LD_{50} value of 54 μM. However, chelidonine showed a significant suppression of hTERT transcription. The quantitative real-time RT-PCR technique estimated the strongest decrease in mRNA level of hTERT in MCF-7 cells 48 h treated with 8 μM chelidonine to 3.5 ± 1.5 % of untreated controls. A reduction of hTERT mRNA level to ~60% and less than 40% of untreated cells was observed when the cells were treated with 0.1 and 1 μM of chelidonine, respectively (Figure 4). Chelerythrine and sanguinarine reduced hTERT transcription to 35 ± 3.2% and 32 ± 3.3% of untreated controls at their respective IC_{50} values.

3.5. Chelerythrine showed the strongest interaction with G4 structure

Thermal FRET analysis of the double-labeled oligonucleotide F21T showed different T_m for G4-alkaloid complexes, indicating that the complexes tested here had different stabilities (Figures 5 and 6B). The T_m values of F21T in 100 mM sodium cacodylate buffer containing 100 mM KCl were calculated at 73°C using dF/dT curves by Rotor-Gene 6.01 software.

The significant high Tm measured for F21T in presence of Chelerythrine and Sanguinarine indicated a strong binding with telomeric G4 structures. Chelerythrine showed the strongest interaction with F21T; as it increased the melting temperature by ~6 °C at equal concentration of F21T and chelerythrine (Figures 5A and 6B green line). Sanguinarine also showed strong binding to F21T, although it was weaker than chelerythrine (Figure 5A and 6B orange line). The ΔT_m caused by sanguinarine on F21T was about 3°C at equimolar concentration. However, berberine, cheldionine and papaverine did not increase the melting temperature of F21T at 1:1 concentration ratio (Figures 5A and 6B; the dark blue, red and blue curves respectively). This suggests a very weak interaction between these alkaloids and F21T. The interaction of the ligands with the unlabeled telo-21G and its stabilization as monitored by $CD_{290\ nm}$ melting shows a similar overall pattern from strong binding to weaker interactions (Figure 6A; the same colors as 5A and 6B). Again chelerythrine shows the strongest interaction, inducing a ΔT_m of 18°C at 100/1 with berberine second at 12°C, both cheldionine and papaverine were the weakest.

3.5.1. G4-duplex transition in the presence of ligands

The specificity of interactions of alkaloids with G-rich F21T oligonucleotide was verified by performing G4-duplex transition experiments in the presence of the complementary oligonucleotide CT22 using a modified thermal FRET method. In these experiments, equimolar solutions of both, F21T and CT22, were first boiled at 95°C for 10 min followed by immediate chilling on ice. Incubating the mixture of oligonucleotides at 37°C allows folding of either duplex or quadruplex structures. A duplex structure will be preferred in the absence of a quadruplex stabilizing ligand. Formation of the folded structure in G-rich strand will be detectable by lower fluorescence intensity than control at the beginning of heating step in FRET measurements. In the absence of any alkaloid, an equimolar mixture of F21T and CT22 showed a sigmoidal curve

starting with high fluorescence intensity at the beginning of FRET measurements (because of flurophore dye separation by duplex formation) followed by a clear transition step, marked as "**a**" (Figure 5A, middle), that correlated with melting temperature of the double helix structure. However, when the strands are separated (at least a fraction of) the G-rich strand F21T oligonucleotide can fold into G4 structure (denoted as "**GQ**" in the curve). By continued heating, a second transition step occurs by denaturing the quadruplexes and if any suitable ligand stabilizes this G4 structure, a ΔT_m will be observed, marked as "**b**" in the curve (Figure 5B, middle).

Folding of F21T in the presence of any ligand will lead to fluorescence quenching. On the other hand, if the ligand strongly interacts with the duplex and stabilizes it, no such quenching will occur and probably a positive ΔT_m is recorded in transition step "a". Meanwhile the ligands that interact with G4 structure may quench fluorescence leading to lower fluorescence intensity, G4 formation in F21T at lower temperature and a negative ΔT_m in transition step "a". This modified FRET-melting method may help to differentiate between quadruplex and duplex specific ligand binding. None of the alkaloids in this study stabilized F21T:CT22 duplex, however chelerythrine and sanguinarine exhibited strong fluorescence quenching at the beginning of the heating and a negative ΔT_m in the transition step "a" (Figure 5A, middle). While other ligands made no changes on both transition steps. Chelerythrine and in a lesser amount sanguinarine increased T_m of F21T as observed in transition step "b". This suggests the stronger effects of these two benzophenanthridine alkaloids on telomeric G4 stabilization.

Chelidonine did not show any considerable changes in melting temperature of F21T, in presence or absence of CT22, although it has previously been shown to inhibit telomerase [12]. Chelerythrine and sanguinarine exhibited a significant stabilization effect on telomeric G4 structure even in the presence of the complementary strand, CT22. In the presence of equimolar concentration of these alkaloids, the fluorescence intensity of F21T largely decreased at the beginning of the heating step of the FRET measurements. The lower fluorescence intensity reasonably correlated with the folded state of F21T quadruplex. Both chelerythrine and sanguinarine strongly favored F21T folding into G4 than hybridizing with CT22 to a duplex DNA. The lowest fluorescence intensity of F21T was detected in the presence of equimolar concentration of chelerythrine and sanguinarine which caused a ~50 and 40% decrease in fluorescence intensity

respectively. Berberine exhibited a weaker quadruplex stabilizing effect than chelerythrine and sanguinarine, while reducing the fluorescence intensity of F21T by about 30%. Papaverine and cheldionine did not show any significant ΔT_m in F21T similar to the classic FRET-melting experiments.

The second transition step "b" was almost the same as observed in classical FRET-melting experiments (without the complementary CT22) and the T_m values are almost the same (it was highlighted with red rectangle for berberine in Figure 5B). In summary these observations support the more selective interaction of chelerythrine than sanguinarine and berberine with telomeric sequences.

3.5.2. Molecular dynamics of telomeric-G4 in complex with isoquinolines

Since no structural data of the studied complexes is available, automated ligand docking and MD simulations were carried out to examine the plausible binding features of the ligands with the G4. The binding energies in kcal/mol, calculated after docking the ligands to the quadruplex were in the following order:

Chelerythrine (-29.5) > Berberine (-25.6) > Sanguinarine (-23.6) > Chelidonine (-19.6) > Papaverine (-16.6)

The final configuration of the systems, after 250 ns MD run revealed that the ligands stacked on the quartet with the chromophore maximizing the π-π stacking interactions. The nitrogen in the ligand molecules exhibited a preference to position on top of central electronegative channel that runs through the G4 (Figure 7). The final results from the MD simulations of the complexes are presented in the Supplementary data section.

3.6. The alkaloids generally inhibited both telomerase and Taq polymerase

Ligand-TRAP assay carried out in the presence of chelerythrine, berberine and sanguinarine showed that the alkaloids inhibited telomerase by varying degrees (Figure 8). The effect was not specific to telomerase as similar effect was observed when the alkaloids were added after telomere elongation, in which only the Taq polymerase was active. Thus both telomerase and Taq

polymerase were inhibited by chelerythrine, sanguinarine and berberine. It suggests that strong interaction of these alkaloids with G-rich telomeric sequences, as seen in thermal FRET experiments, is most likely by interfering with both telomerase and Taq activity. Telomerase inhibition appears after a few rounds of primer extension activity of the enzyme by adding the TTAGGG repeats, which adopts G4 structure. The strong interaction of alkaloids may restrict access to the substrate. However in presence of chelerythrine, telomerase was more inhibited than taq polymerase, as incubation with chelerythrine before substrate extension by telomerase showed less TRAP products than incubation after that (Figure 8). No significant reduction in activity of telomerase and/or Taq polymerase was observed in our ligand-TRAP experiments when incubated with chelidonine (data not shown).

4. Discussion

Discovery of new drugs that are selectively cytotoxic against cancer cells is one of the primary objectives for effective cancer treatment. Natural alkaloids of *Chelidonium majus*, have been reported to induce various cell death mechanisms especially through apoptosis induction [15]. The most important benzylisoquinolines in this plant include chelidonine, sangunarine, chelerythrine, and berberine with slightly different structures and various extents of anti-proliferative effects in cancer cell lines [51-54]. However, more investigation is required to elucidate the detailed mechanisms and structure-function relationship relevant to their antiproliferative effects.

This study has focused on a comparative study of selective binding to G4 DNA and anti-telomerase activity of the main alkaloids of *C. majus*. MTT experiments revealed that all the compounds were cytotoxic in MCF-7 cells. Chelerythrine and sanguinarine were the most cytotoxic alkaloids, while chelidonine having a hydroxyl group exhibited a relatively less cytotoxicity. Papaverine, a benzyl-isoquinoline alkaloid with fewer aromatic rings in its structure and more flexible than berberine, has shown least cytotoxicity (LD_{50} about 120 µM estimated using MTT). Papaverine also has inhibitory effects on telomerase activity and hTERT expression in both MCF-7 [48] and HepG2 [49].

Detection of telomerase activity using a Quantitative TRAP assay revealed a very low-level of telomerase activity in MCF-7 cells treated with chelidonine or sanguinarine. As this assay

measured the enzyme activity in equal amounts of total protein in samples, the reduced activity implies depletion of the relative amount of the active ribonucleoprotein. Telomerase regulation albeit very complicated, is mainly through transcriptional regulation of the catalytic subunit of the enzyme [53]. In the treated MCF-7 cells with chelidonine and sanguinarine, hTERT mRNA levels followed the same diminution as the telomerase activity. Sub-micromolar concentrations of both chelidonine and sanguinarine led to a significant decrease in telomerase activity along with a decrease in hTERT transcription level. Chelerythrine inhibited telomerase by most extent to ~57% of un-treated control cells at its LD_{50} (2.5 μM). Remarkably, berberine showed a significant decrease in telomerase activity to ~16% of untreated cells at 3 μM concentration. It is noteworthy that, in spite of berberine, which is a potent genotoxin and strong DNA intercalator [54-56], no genotoxicity and hepatotoxicity of chelerythrine and sanguinarine has been suggested in animal model up to 5 mg per 1 kg body weight [2, 57].

Another possible mechanism of telomerase inhibition by small molecules is substrate sequestering through G4 stabilization [58, 59]. Our thermal FRET analysis suggests chelerythrine exhibited greatest affinity and specificity among the studied benzophenantridines towards telomeric G4 DNA (Figure 5). It interacted strongly with the synthetic substrate of telomerase and stabilized the folded G4 structure making it inaccessible to the enzyme. G4 structure stabilization was recorded for sanguinarine in a considerably stronger extent than berberine. The ΔT_m of F21T varied considerably in presence of these three alkaloids, although molecular modeling methods suggest almost the similar mode of interactions and comparable binding energies in the hybrid 3+1 topology [64]. Non-electrostatic interactions in the binding of small molecules to G4 are preferable for telomerase inhibition under physiological conditions [60]. Amongst the alkaloids tested here, chelidonine is estimated to have less non-electrostatic interactions than the others as it has an extra hydroxyl group and lesser number of aromatic rings. As thermal FRET analysis did not detect any considerable increase in melting temperature of F21T in presence of chelidonine, direct interference with the telomerase activity by substrate sequestration may not contribute to the inhibition mechanism. In our ligand-TRAP analysis also, no significant change in telomerase and/or Taq polymerase activity was seen after various incubation times with chelidonine. This is consistent with other reports indicating only a minor DNA binding capacity for chelidonine [51]. In conclusion, chelidonine does not interact with telomerase (after ligand-TRAP data) nor does it

sequester its substrate (after thermal FRET data), but strongly inhibited telomerase mainly through hTERT suppression (after qPCR measurments of the hTERT mRNA). Similarly and in agreement with our previous reports [28, 49], papaverine also showed no significant interaction with telomeric quadruplex.

CD experiments confirm the hybrid 3+1 topology of the G4 structures in presence of the studied alkaloids. The ligands showed no considerable changes to enhance the 260 nm peak, while reduced the negative peak at 234 nm. This implies almost a similar mode of interaction of the ligands with F21T and the unlabeled telo-21G.

In conclusion, chelerythrine, sanguinarine and berberine, interfered with telomerase activity by limiting substrate accessibility; while down-regulation of the hTERT gene may also have an important contribution [61]. It is known that several G-rich regions exist in promoter of hTERT [62]. Whether the latter effect is a consequence of G4 interaction with these isoquinolines requires further investigation. These regions are expected to be additional targets for G4 formation in the presence of chelerythrine, sanguinarine and berberine.

Based on thermal FRET observations, the number of fused aromatic rings of the ligands may have the highest impact on the strength of interaction with telomeric quadruplex. So that by reducing the number of the aromatic rings or separating them a smaller ΔT_m will be expected. Inclusion of polar substitutions may decrease the interaction. The benzophenanthridine alkaloids have stronger interaction with telomeric G4 structure than other isoquinolines. Also, opening the methylene dioxy rings may enhance the interactions. This highlights the priority of aromatic and hydrophobic interactions in binding of these ligands to telomeric G-quadruplex.

Acknowledgments

This work was supported by the Iran National Science Foundation (INSF) granted to S.K.N. J.S. acknowledges support by Praemium Academiae, Czech Republic. JS and BI acknowledge support from the Czech Science Foundation (Grant No 16-13721S) and the CEITEC 2020 project (LQ1601) with financial support from the Ministry of Education, Youth and Sports of the Czech Republic under the National Sustainability

Programme II. S.H. would like to thank the UCL School of Pharmacy for the award of a UCL Excellence Fellowship.

Conflicts of Interest

The authors declare that they have no conflict of interests.

References

1. Amin AR, Karpowicz PA, Carey TE, Arbiser J, Nahta R, Chen ZG, Dong JT, Kucuk O, Khan GN, Huang GS, Mi S, Lee HY, Reichrath J, Honoki K, Georgakilas AG, Amedei A, Amin A, Helferich B, Boosani CS, Ciriolo MR, Chen S, Mohammed SI, Azmi AS, Keith WN, Bhakta D, Halicka D, Niccolai E, Fujii H, Aquilano K, Ashraf SS, Nowsheen S, Yang X, Bilsland A, Shin DM. Evasion of anti-growth signaling: A key step in tumorigenesis and potential target for treatment and prophylaxis by natural compounds. Semin. Cancer Biol. 35 (2015) Suppl: S55-77.

2. Franceschin M, Rossetti L, D'Ambrosio A, Schirripa S, Bianco A, Ortaggi G, Savino M, Schultes C, Neidle S. Natural and synthetic G-quadruplex interactive berberine derivatives. Bioorg Med Chem Lett. 16 (2006) 1707-11.

3. Macha MA, Krishn SR, Jahan R, Banerjee K, Batra SK, Jain M. Emerging potential of natural products for targeting mucins for therapy against inflammation and cancer. Cancer Treat Rev. 41 (2015) 277-288.

4. Ghosh S, Pradhan SK, Kar A, Chowdhury S, Dasgupta D. Molecular basis of recognition of quadruplexes human telomere and c-myc promoter by the putative anticancer agent sanguinarine. Biochim Biophys Acta. 1830(2013) 4189-201.

5. Capistrano IR, Wouters A, Lardon F, Gravekamp C, Apers S, Pieters L. In vitro and in vivo investigations on the antitumour activity of *Chelidonium majus*. Phytomed. 22 (2015) 1279-87.

6. Kim DJ, Ahn B , Han BS, Tsuda H. Potential preventive effects of *Chelidonium majus* L. (Papaveraceae) herb extract on glandular stomach tumor development in rats treated with N-methyl-N'-nitro-N nitrosoguanidine (MNNG) and hypertonic sodium chloride. Cancer Lett. 112 (1997) 203–208.

7. Lohninger A, Hamler F. Chelidonium majus L. (Ukrain) in the treatment of cancer patients. Drugs Exp. Clin. Res. 18 (1992) Suppl:73–77.

8. Gilca M, Gaman L, Panait E, Stoian I, Atanasiu A. *Chelidonium majus* – an Integrative Review: Traditional Knowledge versus Modern Findings. Forsch Komplementmed. 17 (2010) 241–248.

9. Colombo ML, Bosisio E. Pharmacological activities of *Chelidonium majus* L. (Papaveraceae). Pharmacol. Res. 33 (1996) 127–34.

10. Habermehl D, Kammerer B, Handrick R, Eldh T, Gruber C, Cordes N. Proapoptotic activity of Ukrain is based on *Chelidonium majus* L. alkaloids and mediated via a mitochondrial death pathway. BMC Cancer. 6 (2006) 14.

11. Huh J, Liepins A, Zielonka J, Andrekopoulos, Kalyanaraman B, Sorokin A. Cyclooxygenase 2 rescues LNCaP prostate cancer cells from sanguinarine-induced apoptosis by a mechanism involving inhibition of nitric oxide synthase activity. Cancer Res. 66 (2006) 3726–3736.

12. Patil JB, Kim J, Jayaprakasha GK. Berberine induces apoptosis in breast cancer cells (MCF-7) through mitochondrial-dependent pathway. Eur J Pharmacol. 645 (2010) 70-8.

13. Noureini SK, Wink M. Transcriptional down regulation of hTERT and senescence induction in HepG2 cells by chelidonine. World J. Gastroenterol. 15 (2009) 3603-10.

14. Kazemi Noureini S., Esmaili H. Multiple mechanisms of cell death induced by chelidonine in MCF-7 breast cancer cell line. Chem. Biol. Interact. 223 (2014) 141–149.

15. Philchenkov A, Kaminsky V, Zavelevich M, Stoika R. Apoptogenic activity of two benzophenanthrid-ine alkaloids form *Chelidonium majus* L. does not correlate with their DNA damaging effects. Toxicol. In Vitro 22 (2008) 287–295.

16. Cordes N, Plasswilm L, Bamberg M, Rodemann HP. Ukrain, An alkaloid thiophosphoric acid derivative of *Chelidonium majus* L. protects human fibroblasts but not human tumor cells in vitro against ionizing radiation. Int. J. Rad. Biol. 78 (2002) 17–27.

17. Hohenwarter O, Strutzenberger K, Katinger H, Liepins A, Nowicky JW. Selective inhibition of in vitro cell growth by the antitumor drug Ukrain. Drugs Exp. Clin. Res. 18(suppl) (1992) 1–4.

18. Huffman KE, Levene SD, Tesmer VM, Shay JW, Wright WE. Telomere shortening is proportional to the size of the G-rich telomeric 3'-overhang. J. Biol. Chem. 275 (2000) 19719-22.

19. Avilion AA, Piatyszek MA, Gupta J, Shay JW, Bacchetti S, Greider CW. Human telomerase RNA and telomerase activity in immortal cell lines and tumor tissues Cancer Res. 56 (1996) 645-50.

20. Hiyama E, Yokoyama T, Tatsumoto N, Hiyama K, Imamura Y, Murakami Y. Telomerase activity in gastric cancer. Cancer Res. 55 (1995) 3258-3262.

21. Smith LL, Coller HA, Roberts JM. Telomerase modulates expression of growth-controlling genes and enhances cell proliferation. Nat. Cell Biol 5 (2003) 474-479.

22. Stewart SA, Weinberg RA. Telomeres: cancer to human aging. Ann. Rev. Cell Dev. Biol. 22 (2006) 531–557.

23. Hwang H, Kreig A, Calvert J, Lormand J, Kwon Y, Daley JM, Sung P, Opresko PL, Myong S. Telomeric overhang length determines structural dynamics and accessibility to telomerase and ALT-associated proteins. Structure. 22 (2014) 842-53.

24. Maji B, Bhattacharya S. Advances in the molecular design of potential anticancer agents via targeting of human telomeric DNA. Chem Commun (Camb). 50 (2014) 6422-38.

25. Joseph I, Tressler R, Bassett E, Harley C, Buseman CM, Pattamatta P, et al. The telomerase inhibitor imetelstat depletes cancer stem cells in breast and pancreatic cancer cell lines. Cancer Res. 70 (2010) 9494-504.

26. Crees Z, Girard J, Rios Z, Botting GM, Harrington K, Shearrow C, Wojdyla L, Stone AL, Uppada SB, Devito JT, Puri N. Oligonucleotides and G-quadruplex stabilizers: targeting telomeres and telomerase in cancer therapy. Curr Pharm Des. 20 (2014) 6422-37.

27. Schultes CM, Guyen B, Cuesta J, Neidle S. Synthesis, biophysical and biological evaluation of 3,6-bis-amidoacridines with extended 9-anilino substituentsas potent G-quadruplex-binding telomerase inhibitors. Bioorg Med Chem Lett. 14(2004) 4347-51.

28. Abachi F, Kazemi Noureini S. Evaluation of natural compounds for telomeric DNA interaction using FRET thermal melting analysis. Clin. Biochem. 44 (2011) 13, S257.

29. Bessi I, Bazzicalupi C, Richter C, Jonker HR, Saxena K, Sissi C, Chioccioli M, Bianco S, Bilia AR, Schwalbe H, Gratteri P.Spectroscopic, molecular modeling, and NMR-spectroscopic investigation of the binding mode of the naturalalkaloids berberine and sanguinarine to human telomeric G-quadruplex DNA. ACS Chem Biol. 7(2012) 1109-19.

30. Bhadra K, Maiti M, Kumar GS.DNA-binding cytotoxic alkaloids: comparative study of the energetics of binding of berberine, palmatine, andcoralyne. DNA Cell Biol. 27 (2008) 675-85.

31. Bessi I,Bazzicalupi C, Richter C, Jonker HR, Saxena K, Sissi C, Chioccioli M, Bianco S, Bilia AR, Schwalbe H, Gratteri P. Spectroscopic, Molecular Modeling, and NMR-Spectroscopic Investigation of the Binding Mode of the Natural Alkaloids Berberine and Sanguinarine to Human Telomeric G-Quadruplex DNA. ACS Chem Biol. 7 (2012) 1109-19.

32. Mosmann T. Rapid colorimetric assay for cellular growth and survival; application to proliferation and cytotoxicity assays. J Immunol Methods. 65 (1983) 55-63.

33. Kim NW, Piatyszek MA, Prowse KR, Harley CB, West MD, Ho PL. Specific association of human telomerase activity with immortal cells and cancer. Science. 266 (1994) 2011-50.

34. Bradford MM. A rapid and sensitivi method for quantific).For each of control and/in utilizing the principle of protein-dye binding. Anal Biochem. 72 (1976) 248-254.

35. Hou M, Dawei X, Byorkltolm M, Gruber A. Real-Time quantitative telomeric repeat amplitication protocol Assay for the detection of telomerase activity. Clin Chemistry. 47 (2001) 519-24.

36. Noureini SK, Wink M. Antiproliferative effects of crocin in HepG2 cells by telomerase inhibition and hTERT down-regulation. Asian Pac. J. Cancer Prev. 13 (2012) 2305-9.

37. Kazemi Noureini S, Tanavar F. Boldine, a natural aporphine alkaloid, inhibits telomerase at non-toxic concentrations. Chem. Biol. Interact. 231 (2015) 27-34.

38. Guédin A, Lacroix L, MergnyJL. Thermal Melting Studies of Ligand DNA Interactions Drug-DNA Interaction Protocols. Methods Mol. Biol. 613 (2010) 25-35.

39. Ohnmacht SA, Neidle S. Small-molecule quadruplex-targeted drug discovery. Bioorg Med Chem Lett. 24 (2014) 2602–2612.

40. Katritch, V., Totrov, M. & Abagyan, R. ICFF: a new method to incorporate implicit flexibility into an internal coordinate force field. J. Comp. Chem. 24 (2003) 254-265.

41. Case DA, Berryman JT, Betz RM, Cerutti DS, Cheatham TE, Darden TA, Duke RE, Giese TJ, Gohlke H, Goetz AW, Homeyer N, Izadi S, Janowski P, Kaus J, Kovalenko A, Lee TS, LeGrand T, Li P, Luchko T, Luo R, Madej B, Merz KM, Monard G, Needham P, Nguyen H, Nguyen HT, Omelyan I, Onufriev A, Roe DR, Roitberg A, Salomon-Ferrer R, Simmerling CL, Smith W, Swails J, Walker RC, Wang J, Wolf RM, Wu X, York DM and Kollman PA (2015), AMBER 2015, University of California, San Francisco.

42. Perez, A. Marchán I, Svozil D, Sponer J, Cheatham TE 3rd, Laughton CA, Orozco M. Refinement of the AMBER force field for nucleic acids: improving the description of alpha/gamma conformers. Biophys. J. 92 (2007) 3817–3829.

43. Krepl, M. Zgarbová M, Stadlbauer P, Otyepka M, Banáš P, Koča J, Cheatham TE 3rd, Jurečka P, Sponer J. Reference simulations of noncanonical nucleic acids with different chi variants of the AMBER force field: quadruplex DNA, quadruplex RNA and Z-DNA. J. Chem. Theory Comput. 8 (2012) 2506–2520.

44. Cornell WD, Cieplak P, Bayly CI, Gould IR, Merz KM, Ferguson DM, Spellmeyer DC, Fox T, Caldwell JW, Kollman PA. A 2nd generation force-field for the simulation of proteins, nucleic acids and organic-molecules. J. Amer. Chem. Soc. 117 (1995) 5179–5197.

45. Joung IS and Cheatham TE Determination of Alkali and Halide Monovalent Ion Parameters for Use in Explicitly Solvated Biomolecular Simulations. J. Phys. Chem. B112 (2008) 9020–9041.

46. Harvey, MJ, Giupponi G, and Fabritiis GD, ACEMD: Accelerating Biomolecular Dynamics in the Microsecond Time Scale. J. Chem. Theo. Comp. 5 (2009) 1632-1639

47. Humphrey W, Dalke A and Schulten K, VMD: Visual molecular dynamics. J. Mol. Graphics. 14 (1996) 33-38.

48. Noori ZS., Kazemi Noureini S., Nabiuni M. Investigation of Telomerase activity and hTERT gene expression in MCF7 cells treated with papaverine. Journal of Sabzevar University of Medical Sciences. 20 (2013) 122-132.

49. Kazemi Noureini S., Wink M. Antiproliferative Effect of the Isoquinoline Alkaloid Papaverine in Hepatocarcinoma HepG-2 Cells — Inhibition of Telomerase and Induction of Senescence Molecules. 19 (2014) 11846-59.

50. De Rache A, Mergny JL. Assessment of selectivity of G-quadruplex ligands via an optimized FRET melting assay. Biochimie. 115 (2015) 194-202.

51. Kaminskyy V, Zavelevich M, Stoika R. Apoptogenic activity of two benzophenanthridine alkaloids from Chelidonium majus L. does not correlate with their DNA damaging effects. Toxicol. In Vitro. 22 (2008) 287-95.

52. Lu JJ, Bao JL, Chen XP, Huang M, Wang YT. Alkaloids Isolated from Natural Herbs as the Anticancer Agents. Evid Based Complement Alternat Med 2012 (2012) 485042.

53. Counter CM, Meyerson M, Eaton EN, Ellisen LW, Caddle SD, Haber DA. Telomerase activity is restored in human cells by ectopic expression of hTERT (hEST2), the catalytic subunit of telomerase. Oncogene. 16 (1998) 1217–1222.

54. Pasqual MS, Lauer CP, Moyna P, Henriques JA. Genotoxicity of the isoquinoline alkaloid berberine in prokaryotic and eukaryotic organisms. Mutat. Res. 286 (1993) 243-52.

55. Wang Y, Liu Q, Liu Z, Li B, Sun Z, Zhou H, Zhang X, Gong Y, Shao C. Berberine, a genotoxic alkaloid, induces ATM-Chk1 mediated G2 arrest in prostate cancer cells. Mutat Res. 734 (2012) 20-29.

56. Kosina P, Walterová D, Ulrichová J, Lichnovský V, Stiborová M, Rýdlová H, Vičar J, Krečman V, Brabec MJ, Šimánek V. Sanguinarine and chelerythrine: assessment of safety on pigs in ninety days feeding experiment. Food Chem. Toxicol. 42 (2004) 85–91.

57. Berardinelli F, Siteni S, Tanzarella C, Stevens MF, Sgura A, Antoccia A. The G-quadruplex-stabilising agent RHPS4 induces telomeric dysfunction and enhances radiosensitivity in glioblastoma cells. DNA Repair. 25 (2015) 104–115.

58. Salem AA, El Haty IA, Abdou IM, Mu Y. Interaction of human telomeric G-quadruplex DNA with thymoquinone. A possible mechanism for thymoquinone anticancer effect. Biochim Biophys Acta. 1850 (2015) 329–342.

59. Nielsen MC, Larsen AF, Abdikadir FH, Ulven T. Phenanthroline-2,9-bistriazoles as selective G-quadruplex ligands. Eur. J. Med. Chem. 72 (2014) 119–126.

60. Xiong Y-X, Huang Z-H, Tan J-H. Targeting G-quadruplex nucleic acids with heterocyclic alkaloids and their derivatives. Eur J Med Chem. 7 (2015) 538-551.

61. Yaku H, Murashima T, Tateishi-Karimata H, Nakano S, Miyoshi D, Naoki Sugimoto N. Study on effects of molecular crowding on G-quadruplex-ligand binding and ligand-mediated telomerase inhibition. Methods. 64 (2013) 19-27.

62. Lim KW, Lacroix L, Yue DJ, Lim JK, Lim JM, Phan AT. Coexistence of two distinct G-quadruplex conformations in the hTERT promoter. J Am Chem Soc. 132 (2010) 12331-42.

63. Parkinson GN, Lee MP, Neidle S. Crystal structure of parallel quadruplexes from human telomeric DNA. Nature. 417 (2002) 876-80.

64. Chung WJ, Heddi B, Tera M, Iida K, Nagasawa K and Phan AT. Solution structure of an intramolecular (3+1) human telomeric g-quadruplex bound to a telomestatin derivative. J. Am. Chem. Soc. 135 (2013) 13495-13501

65. Zhou J, Fleming A, Averill A, Burrows C and Wallace SS. The NEIL glycosylases remove oxidized guanine lsions from telomeric and promoter quadruplex DNA structures. Nucleic Acids Res. 43 (2015) 8:4039-4054

Figure Legends

Figure 1: Chemical structures of berberine, chelidonine, chelerythrine, sanguinarine, and papaverine.

Figure 2: Cell viability of MCF7 cells after 24 (light gray), 48 (gray) and 72 (black) hours treatment with different concentrations of berberine, chelerythrine, chelidonine and sanguinarine as estimated by MTT. Mean values ± standard error of means is shown.

Figure 3: CD spectra of telo-21G at 1 μM concentration in 10 mM sodium cacodylate buffer and 100 mM KCl pH 7.2 alone (purple) and in the presence of an increasing ligand concentration of chelerythrine, sanguinarine, berberine, chelidonine and papaverine represented by green, black, red, blue, yellow curves respectively at ratios 1:1 (A), 10:1 (B), 100:1 (C) (ligand/ telo-21G. (D) Chelerythrine in the presence of telo-21G at 0.25 and 0.5 μM (2:1, 4:1) in light green, and dark green lines respectively.

Figure 4: Telomerase activity (grey line) and hTERT mRNA level (black line) estimated using q-TRAP and real-time PCR in MCF-7 cells after 48h treatment with the alkaloids. The mean value ± SEM of four logical repeats, each including at least three samples for different concentrations has been presented.

Figure 5A: **Top:** Classical thermal FRET analysis of F21T in 10mM sodium cacodylate, pH 7.2 and 100 mM K+ alone (black) or equimolar concentration of **Ber**berine (dark blue), **Che**lidonine (red), **Chele**rythrine (green), **Pap**averine (blue) and **San**guinarine (orange). **Middle:** t-FRET melting measurements of F21T in the same buffer mentioned above and presence of equimolar concerntation of the complementary oligonucleotide CT22. Its shows two tandem sigmoid curves starting with high fluorescence intensity at the beginning of FRET measurements where F21T:CT22 may form double stranded duplex DNA followed by a clear transition step, marked as "a". By increasing temperature F21T will be released and may fold into G4 structure (GQ). By continuing heating, a second transition step occurs due to denaturation of the quadruplexes, marked as "b", until the G-rich strand is also completely unfolded. **Bottom:** tFRET melting measurements of F21T in 10mM sodium cacodylate, pH 7.2 and 100 mM KCl in presence of

equimolar concentration of the complementary oligonucleotide CT22 and 1:1 concentration ratio of alkaloids as above. Note the similar pattern of this second sigmoidal (boxed rectangle) with the classic FRET melting curve illustrated above.

Figure 5B: (**Left**) Classical FRET melting of 0.25 μM F21T (black) in 10mM sodium cacodylate, pH 7.2 and 100 mM KCl alone (blue) or in presence of 1:1 (red) , 10:1 (green) and 100:1 (purple) ratios of berberine, chelerythrine, chelidonine, papaverine and sanguinarine. (**Middle**) Transition FRET (tFRET) melting analysis of equimolar concentration of F21T and CT22 (0.25 μM each) in 10 mM and 100mM sodium cacodylate without any alkaloid (black) or in presence of 1:1 (red) , 10:1 (green) and 100:1 (violet) ratios of berberine, chelerythrine, chelidonine, papaverine and sanguinarine. (**Right**) Classical thermal $CD_{290\ nm}$ melt analysis of telo-21G at 1 μM in 10 mM sodium cacodylate and 100 mM KCl in presence of final concentrations of 0, 1, 10, and 100 μM ligands (0:1, 1:1,10:1, 100:1 ligand/ telo-21G) in blue, red, green, purple lines respectively.

Figure 6: (A) The difference in $T_{1/2}$ of telo-21G in $CD_{290\ nm}$ melting test and (B) F21T in classical FRET melting in sodium cacodylate buffer, pH 7.2 and 100 mM KCl and in presence of increasing concentrations of alkaloids.

Figure 7: Conformations of the alkaloids when bound to 3+1 hybrid topology G4 DNA [64]. The central nitrogen in Chelerythrine (green), berberine (yellow), chelidonine (black), sanguinarine (red) and papaverine (blue) orients on top of the electronegative channel in the quadruplex structure. The side view of how all ligands bind is illustrated in the bottom right corner.

Figure 8: Ligand-TRAP measurements. A master mix of q-TRAP reaction including MCF-7 cell lysate was prepared and aliquoted to two sets on ice. Various concentrations of the desired alkaloid berberine, chelerythrine and sanguinarine were added as explained in part 2.3. Treatments in 1, 3 and 5 have been done before primer elongation by telomerase and in 2, 4 and 6 before q-PCR. In samples 1, 3 and 5 both telomerase and hot-start Taq polymerase have been exposed to the alkaloids while in samples 2, 4 and 6 only hot-start Taq enzyme has been exposed to the alkaloids.

Figure1

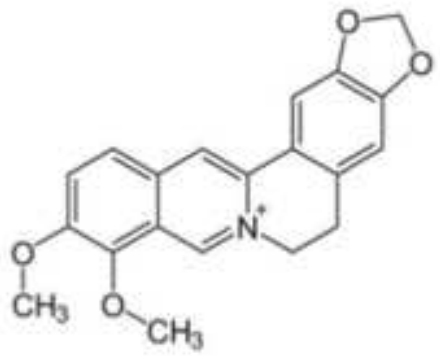

berberine

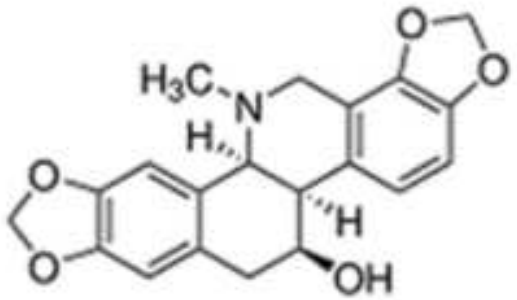

chelidonine

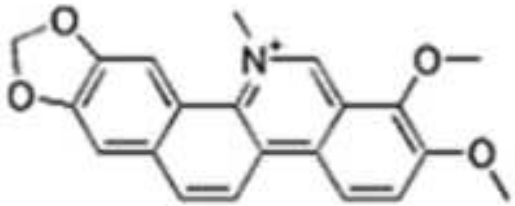

chelerythrine

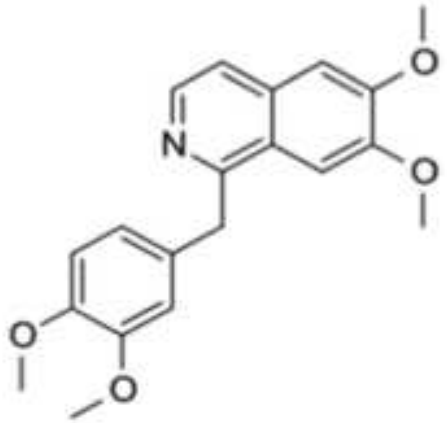

papaverine

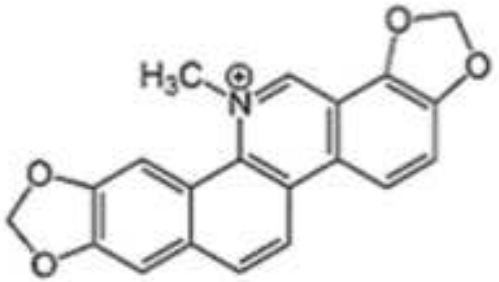

sanguinarine

Figure2

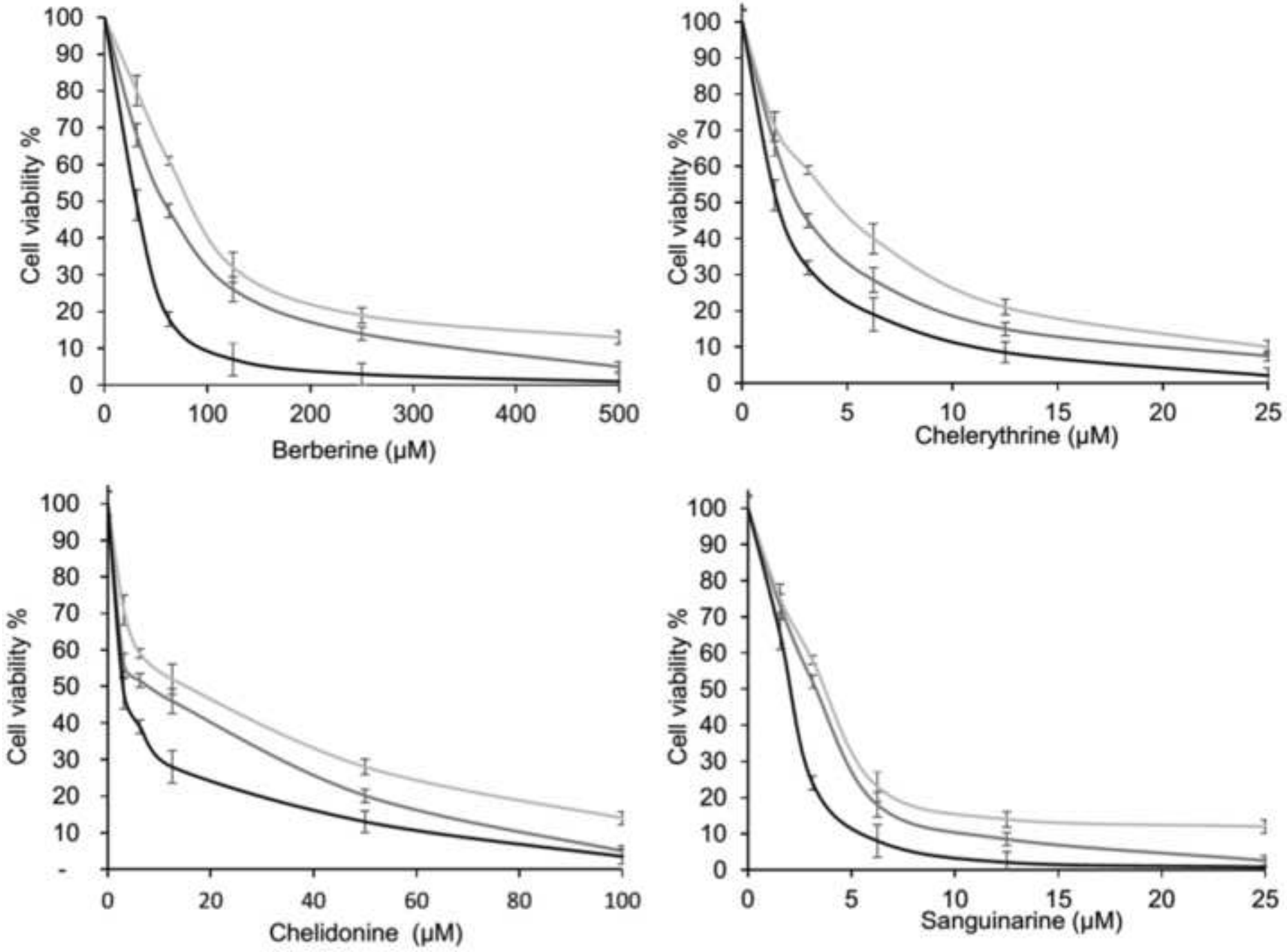
Cell viability %
Berberine (μM)
Chelerythrine (μM)
Chelidonine (μM)
Sanguinarine (μM)

Figure3

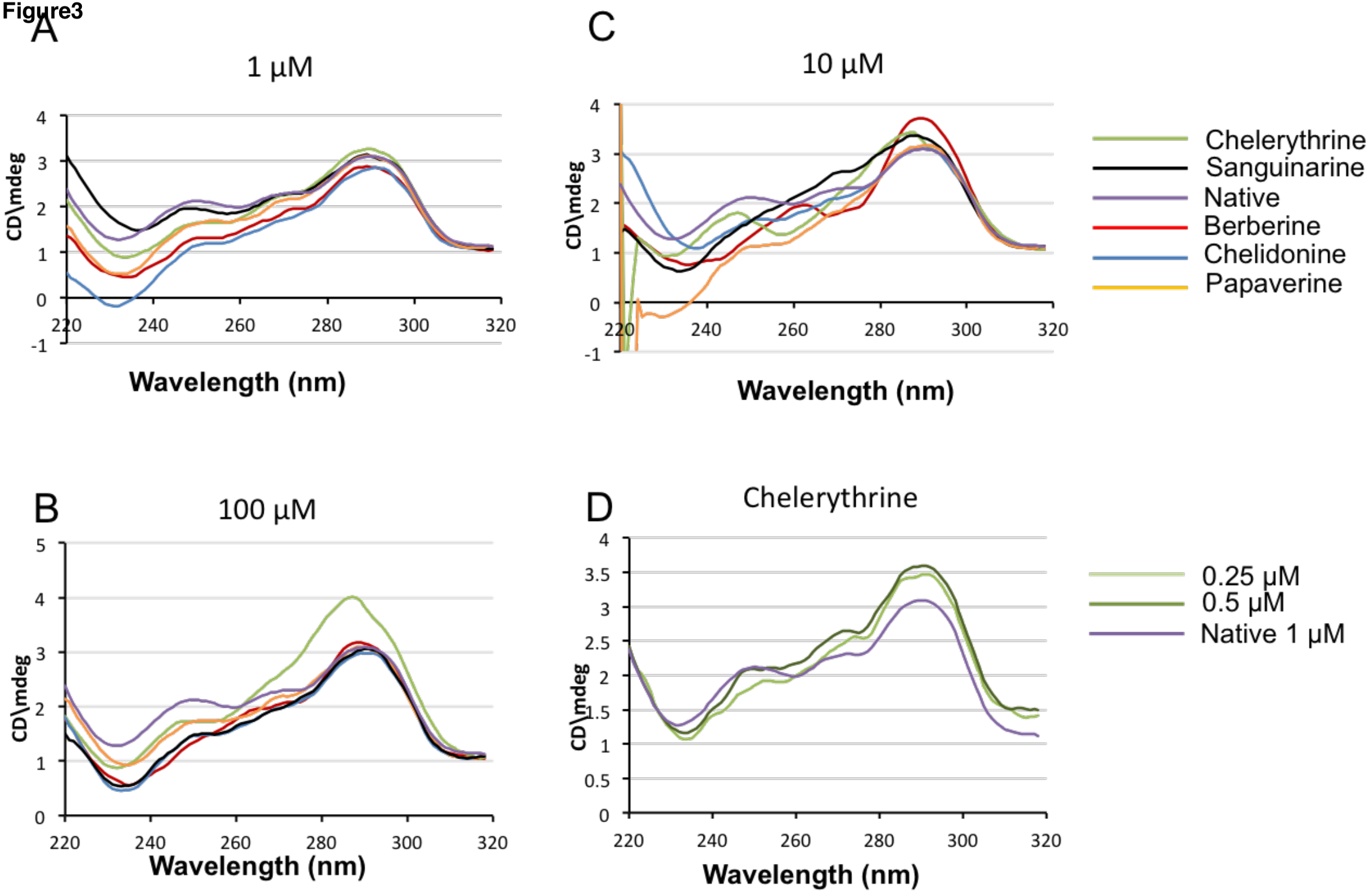
A
1 µM
CD\mdeg
Wavelength (nm)
C
10 µM
CD\mdeg
Wavelength (nm)
Chelerythrine
Sanguinarine
Native
Berberine
Chelidonine
Papaverine
B
100 µM
CD\mdeg
Wavelength (nm)
D
Chelerythrine
CD\mdeg
Wavelength (nm)
0.25 µM
0.5 µM
Native 1 µM

Figure4

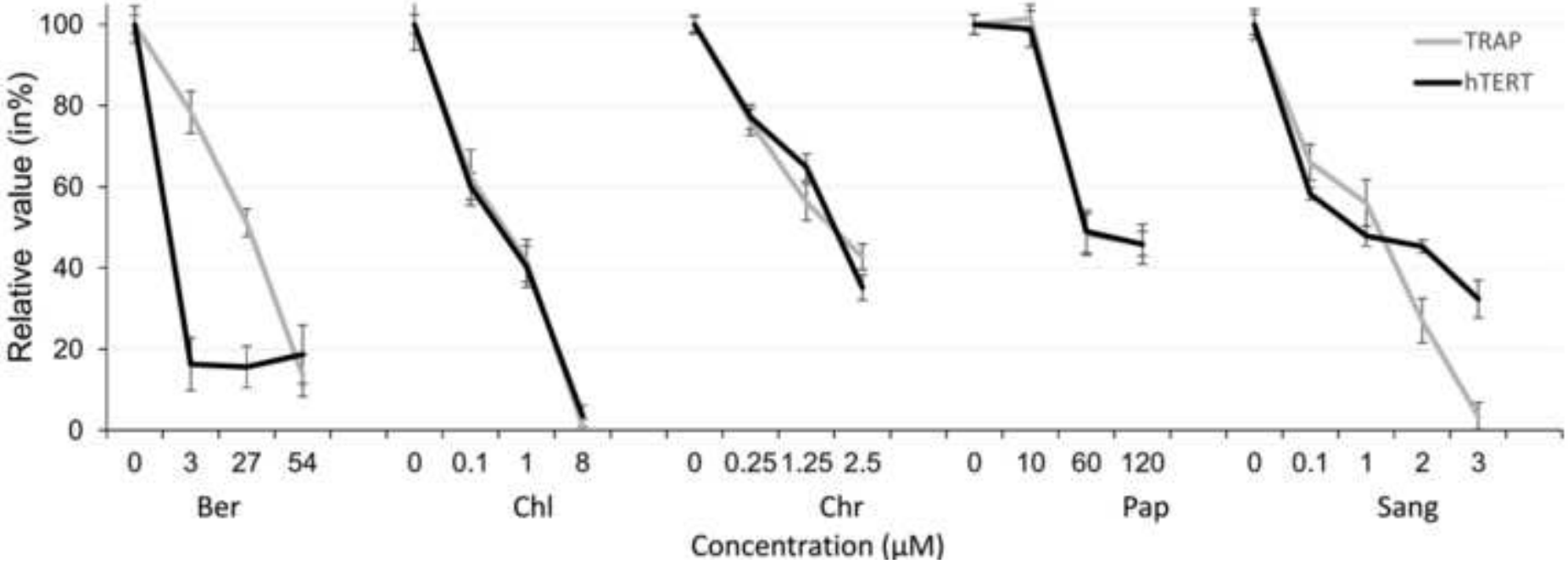
Relative value (in%)
100
80
60
40
20
0
TRAP
hTERT
0 3 27 54
Ber
0 0.1 1 8
Chl
0 0.25 1.25 2.5
Chr
0 10 60 120
Pap
0 0.1 1 2 3
Sang
Concentration (μM)

Figure5

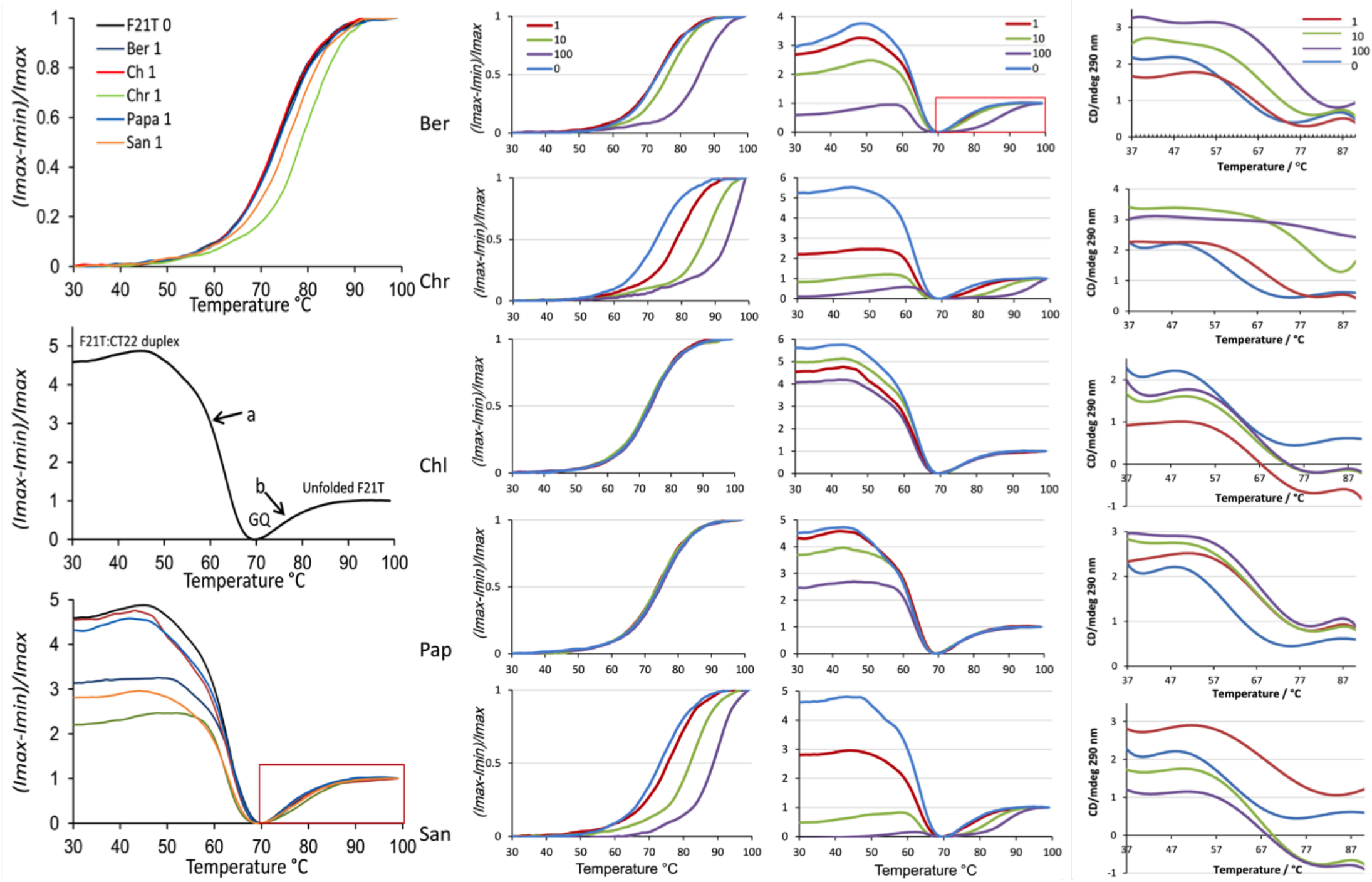
A
B
classic FRET melting
tFRET melting
thermal CD290nm
F21T 0
Ber 1
Ch 1
Chr 1
Papa 1
San 1
(Imax-Imin)/Imax
Temperature °C
Ber
Chr
Chl
Pap
San
F21T:CT22 duplex
a
b
GQ
Unfolded F21T
1
10
100
0
CD/mdeg 290 nm
Temperature / °C

Figure6

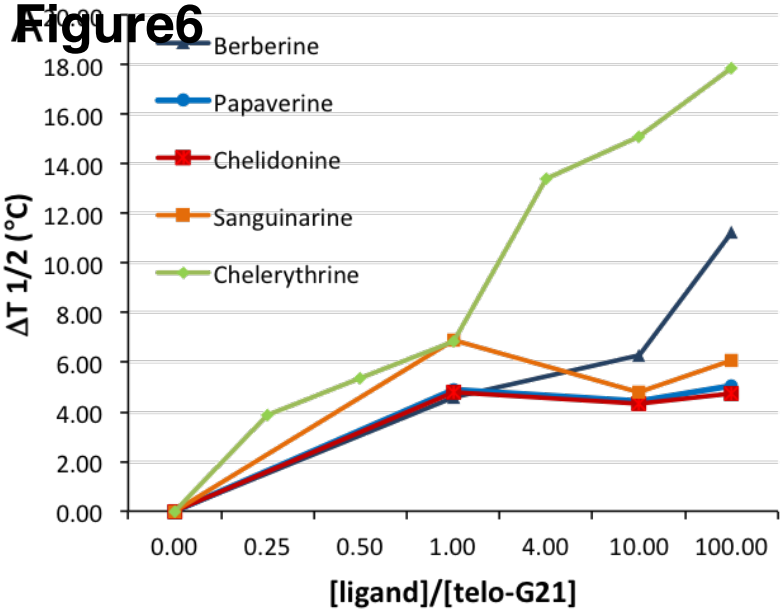
Berberine
Papaverine
Chelidonine
Sanguinarine
Chelerythrine
ΔT 1/2 (°C)
0.00
2.00
4.00
6.00
8.00
10.00
12.00
14.00
16.00
18.00
0.00
0.25
0.50
1.00
4.00
10.00
100.00
[ligand]/[telo-G21]

B

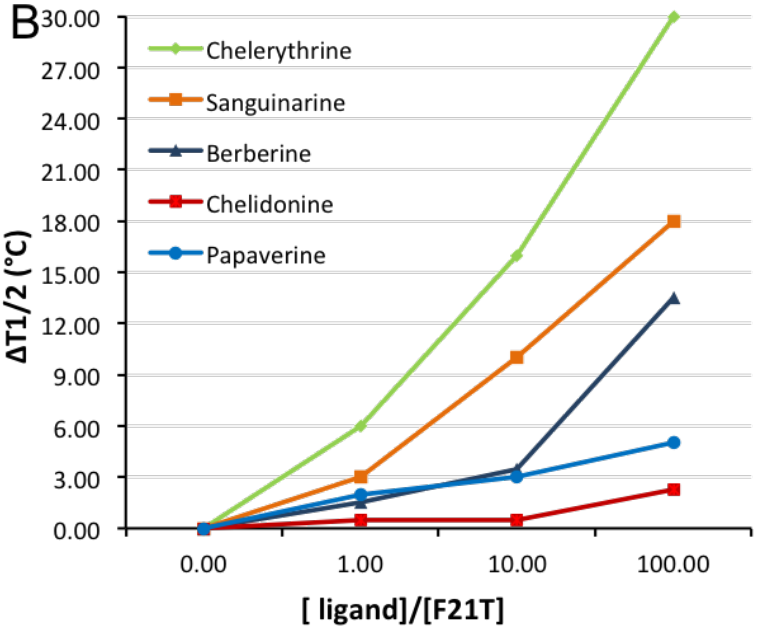
Chelerythrine
Sanguinarine
Berberine
Chelidonine
Papaverine
ΔT1/2 (°C)
0.00
3.00
6.00
9.00
12.00
15.00
18.00
21.00
24.00
27.00
30.00
0.00
1.00
10.00
100.00
[ligand]/[F21T]

Figure7

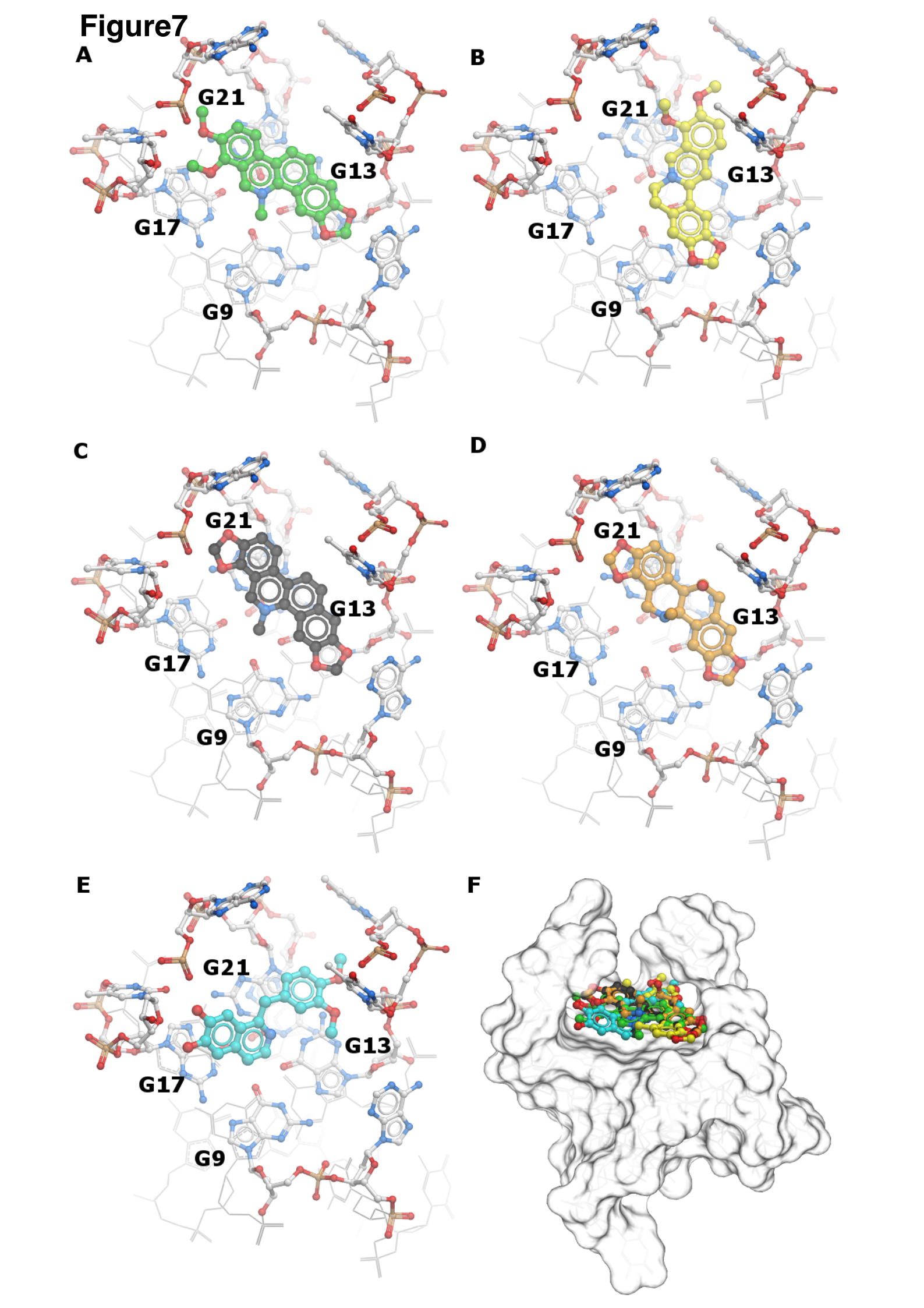
A
G21
G13
G17
G9
B
G21
G13
G17
G9
C
G21
G13
G17
G9
D
G21
G13
G17
G9
E
G21
G13
G17
G9
F

Figure8

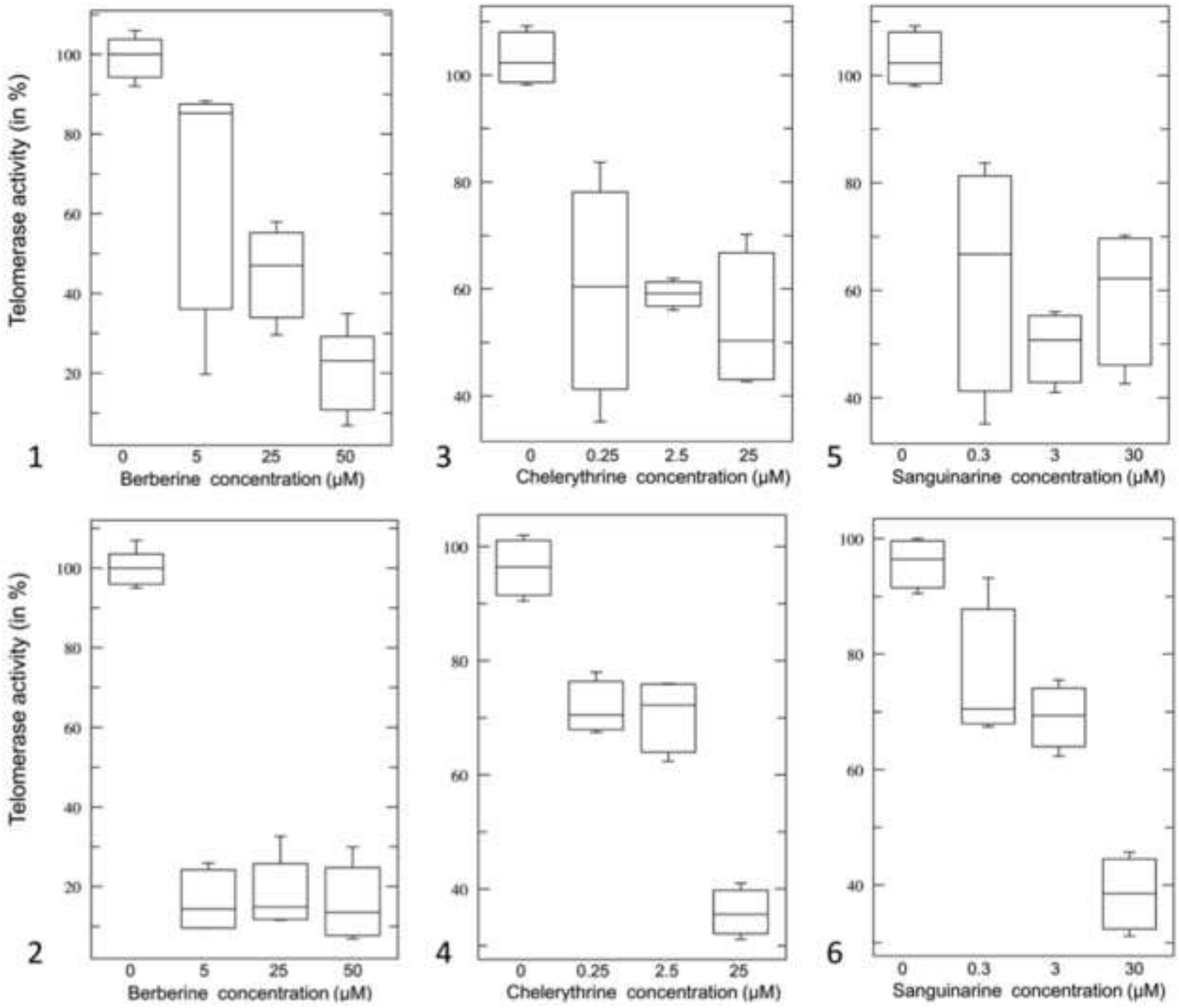
Telomerase activity (in %)
100
80
60
40
20
1
0
5
25
50
Berberine concentration (μM)
2
Berberine concentration (μM)
3
0
0.25
2.5
25
Chelerythrine concentration (μM)
4
Chelerythrine concentration (μM)
5
0
0.3
3
30
Sanguinarine concentration (μM)
6
Sanguinarine concentration (μM)

Supplementary Section

Quantitative Telomere Repeat Amplification Protocol (q-TRAP)

Briefly, a master mix of q-TRAP reaction including MCF-7 cell lysate was prepared and aliquoted to two sets on ice (A and B). Various concentrations of the desired alkaloid were added to samples of set A and incubated for 30 minutes on ice. Then all samples of both sets were incubated for 20 minutes at 24°C for extending TS primer by telomerase. All the samples were put back on ice and the same concentrations of alkaloid as set A was added to the samples of set B. Only Taq polymerase may be affected in this set. The amplification and quantification were done as described in the previous section. This experiment has been repeated at least three times, and each repeat included triplicate samples for each concentration of the alkaloid. Traces of RNase contamination that potentially can give rise to false positive results was checked by incubating total RNA with aliquots of the alkaloids for 0 or 30 minutes at room temperature followed by electrophoresis in agarose gel.

Table 1. Time table of incubations and treatments in various sets of ligand TRAP test.

Time from start point (min)	**0**	**30-50**	**50**	**50-150**
Set	**Incubation on ice**	**Telomerase activity at 24°C**	**Incubation on ice**	**Amplification of telomerase products (q-PCR)**
A	Treatment with the alkaloid		-	
B	-		Treatment with the alkaloid	

Molecular Dynamics Simulations

The ligands studied here display a common mode of binding. The rings of the ligands are able to interact via π-π stacking at the exposed surface of the quadruplex.

Chelerythrine: In the starting structure, the rings of the ligand stack with the G13 and G21 of the quadruplex and the nitrogen of the ring align along the cation channel of the quadruplex. During the simulation the ligand stacks on half of the quartet, aligning the nitrogen along the central axis of the quadruplex.

Berberine: The ligand has a large surface area and stacks with G13 and G21 from the top quartets. The central nitrogen atom in the ring of ligand is aligned along the channel cavity of the quadruplex and anchors the ligand. The π-π stacking between the ligand-quadruplex is stable throughout the simulation, with the ligand moving around the anchor.

Sanguinarine: The rings of the ligand stack with the quartets such that the nitrogen is positioned over the central electronegative channel. During the course of the simulation the ligand is able to stack above G13 and G21 of the quartet.

Chelidonine: In the quadruplex-chelidonine structure, the aromatic rings stacks on one half of the top quartet. During the simulation, the ligand shifts to stack with G13 and G21 bases similar to the orientation of Chelerythrine.

Papaverine: During the simulation, ligand is oriented in such a way that the isoquinoline rings stack partially on the top quartet. The nitrogen in the isoquinoline ring is positioned on the central channel. The flexiblity around the central methyl linker permits partial stacking of the phenyl ring on G21 of the top quartet.